Mineralium Deposita (1998) 33: 59–81

ARTICLE

J.M. Leistel · E. Marcoux · Y. Deschamps

Chert in the Iberian Pyrite Belt

Received: 11 March 1996 / Accepted: 9 April 1997

Abstract Since lenses of chert are common within the volcano-sedimentary succession hosting the massive sulphide deposits of the Iberian Pyrite Belt (Spain and Portugal), we examined numerous chert occurrences, both petrographically and geochemically, to test their possible value for massive sulphide exploration. The chert is found at two main lithostratigraphic levels (upper and lower) that are also interpreted as massive-sulphide bearing. In both cases the chert is located at the top of acidic volcanic sequences or in the associated sediments; we have not been able to observe the relationships between massive sulphides and chert, but some of the large orebodies of the Province (Lousal, La Zarza, Tharsis, Planes-San Antonio body of Rio Tinto, Neves) are described as being locally capped by chert facies. Four main types are recognized among the chert and associated facies: (1) red hematitic chert ± magnetite; (2) radiolarian and/or sedimentary-textured (conglomeratic) chert with hematite and/or Mn oxides; (3) pale sulphidic chert; (4) rhodonite and/or Mn carbonate ± magnetite facies. In the Spanish part of the Province the radiolarian chert is confined to the upper level; the distribution of the other types appears to be haphazard. The hydrothermal origin of the South Iberian chert is shown by its high Fe-Mn and low Co-Ni-Cu contents. The presence of small positive Ce anomalies indicates a shallow marine environment (shelf or epicontinental sea), which is consistent with the volcanological and sedimentological data. The chert was emplaced below the sea floor through chemical precipitation and/or through alteration and replacement of the country rock, residual traces of which are ghost phenocrysts and high Al, Ti and rare earth contents. Macro- and microscopic relationships indicate that the oxide facies (hematite ± magnetite) formed first, probably providing a protective insulating cover against the marine environment and enabling an evolution towards sulphide facies; a phase of Mn carbonate and silicate + quartz ± chlorite + sulphides appears to be even later. It was not possible, through discrimination, to isolate a chert that could be considered as representing a lateral marker of massive sulphides; moreover, both field observations and geochemical data seem to indicate a relative independence of this siliceous sulphide hydrothermal activity from the hydrothermal activity giving rise to the massive sulphides. Such is also indicated by the lead isotopic signature of the chert, which is appreciably more radiogenic than that of the massive sulphides; the lead enrichment in the sulphidic chert facies indicates the participation of a different source (sediments, sea water) from that of the massive sulphides. The hypothesis of an independent hydrothermal "chert" event can thus be envisaged, wherein the chert reflects submarine low-temperature hydrothermal activity that is most apparent during a "break" within the volcano-sedimentary succession and which may locally have competed with the high-temperature hydrothermal activity giving rise to the massive sulphides. The interest of the chert thus rests in its palaeodynamic significance, as a marker of periods of volcanic quiescence, and in its possible role as a protective insulating cap favourable to the deposition of massive sulphides.

Resumen (translated by E. Pascual) Dado que los lentejones de chert son comunes dentro de la sucesión vulcanosedimentaria que contiene los depósitos de sulfuros masivos de la Faja Pirítica Ibérica (España y Portugal), se han examinado numerosos afloramientos de chert, tanto desde un punto de vista petrográfico como geoquímico, para verificar su posible utilidad en la exploración de sulfuros masivos. El chert se encuentra en dos niveles litoestratigráficos principales (superior

Editorial handling: DR

J.M. Leistel · E. Marcoux (✉)
BRGM, DR/DMG, BP6009, 45060 Orléans Cedex 02, France

Y. Deschamps
Seiemsa, Ed. Foro de Somosaguas, Pl.1A, mod. 5–6,
Centra Carabanchel a Pozuelo, Urb. Pinar de Somosaguas,
Pozuelo de Alarcon, 28228 Madrid, Spain

e inferior) que también son interpretados como portadores de mineralizaciones. El chert se localiza en los dos casos en el techo de las secuencias volcánicas ácidas o en los sedimentos asociados. No hemos podido observar las relaciones entre sulfuros masivos y chert, pero se ha descrito que algunas de las mayores masas de la provincia (Lousal, La Zarza, Tharsis, Planes-San Antonio en Ríotinto, Neves) están localmente recubiertas por facies de chert. Se han reconocido cuatro tipos principales entre los cherts y facies asociadas: 1) chert hematítico rojo ± magnetita; 2) chert de radiolarios y/o con textura sedimentaria (conglomerático), con hematites y/o óxidos de manganeso; 3) chert pálido sulfurado; 4) facies con rodonita y/o carbonatos de Mn ± magnetita. En la parte española de la provincia el chert de radiolarios sólo aparece en el nivel superior, en tanto que la distribución de los otros tipos parece aleatoria. El origen hidrotermal del chert sudibérico se refleja en su alto contenido en Fe-Mn y en su escasa abundancia en Co-Ni-Cu. La presencia de pequeñas anomalías positivas de Ce indica un ambiente marino somero (plataforma o mar epicontinental), lo que concuerda con los datos vulcanológicos y sedimentológicos. El chert se emplazó bajo el fondo marino por precipitación química y/o alteración y reemplazamiento de la roca huésped, de la cual quedan trazas, como fantasmas de fenocristales y altos contenidos en Al, Ti y tierras raras. Las relaciones macro y microscópicas indican que primero se formaron las facies de óxidos (hematites ± magnetita), proporcionando una cubierta protectora aislante frente al ambiente marino y favoreciendo la evolución hacia sulfuros masivos. La facies de carbonatos y silicatos de Mn + cuarzo ± clorita + sulfuros parece ser aún más tardía. No ha sido posible discriminar un chert que se pueda considerar representativo como marcador lateral de sulfuros masivos. Además, tanto las observaciones de campo como los datos geoquímicos parecen indicar una relativa independencia de esta actividad hidrotermal silícea respecto de la actividad hidrotermal que produce los sulfuros masivos. Así lo indica también la signatura isotópica de plomo del chert, que es apreciablemente más radiogénica que la de los sulfuros masivos. El enriquecimiento en plomo de la facies de chert sulfurado indica la participación de una fuente diferente de la de los sulfuros masivos (sedimentos, agua marina). Por tanto, debe ser contemplada la hipótesis de un chert hidrotermal independiente, en la cual el chert refleja actividad hidrotermal submarina de baja temperatura, que se hace más evidente durante una ''ruptura'' en la sucesión vulcanosedimentaria, pero que puede haber competido localmente con la actividad hidrotermal de alta temperatura que da origen a los sulfuros masivos. Así, el interés del chert estriba en su significado paleodinámico como marcador de los periodos volcánicos de calma y en su posible papel como cobertura protectora aislante, favorable al depósito de sulfuros masivos.

Introduction

All the theoretical models describing volcano-sedimentary massive sulphides include the presence of exhalite or siliceous tuffite beds, generally located at the top of the sulphide mass and extending out laterally (Large 1977; Klau and Large 1980; Franklin et al. 1981). These beds could thus form a useful stratigraphic marker for the mineral exploration geologist (Scott et al. 1983; Kalogeropoulos and Scott 1983; Liaghat and MacLean 1992). Such siliceous facies (chert), commonly manganiferous, abound in the volcano-sedimentary succession hosting the massive sulphides of the Iberian Pyrite Belt, to such an extent that they cannot all be considered as lateral stratigraphic markers of the sulphide mineralization (Barriga 1990). To determine the exact significance of the siliceous, or chert, layers and to test their usefulness for mineral exploration, we undertook a typological, mineralogical and geochemical study of a large number of exposures reflecting a wide range of contexts throughout the Province in both Spain and Portugal.

Regional geological setting

The South Iberian massive-sulphide Province forms part of the South Portuguese Zone at the southern edge of the Iberian Hercynian belt (Fig. 1). It comprises three conformable successions: (1) a phyllite and quartzite succession (PQ) of Late Devonian age; (2) a volcano-sedimentary succession (VS) of late Famenian to late Visean age; and (3) a Culm succession of greywacke, pelite and conglomerate (Culm) of late Visean to Westphalian age (Schermerhorn 1971; Oliveira 1990). The major structure, considered to be Hercynian, has an average W-E trend and is marked by major kilometre-size folds overturned to the south, a main axial-plane cleavage and numerous south-verging thrust planes (Silva et al. 1990).

The volcano-sedimentary succession (VS) (see Leistel et al. 1997 for a lithostratigraphic column), which hosts massive sulphides and chert, comprises several acidic and basic volcanic and subvolcanic units intercalated in pelite and defining a bimodal suite derived from a continental basic tholeiitic magma and an acidic calc-alkaline magma (Munhá 1983; Thiéblemont et al. 1994). Three successive acidic volcanic events (VA1, VA2 and VA3) are generally distinguished, forming very varied facies: lavas, domes, pyroclastic rocks, and subvolcanic rocks. A marker horizon of purple schist marks the end of the VA2 event and precedes the VA3 event, which represents the last volcanic activity of the VS succession. The sulphide mineralization and the chert, as well as associated Mn carbonate and silicate facies, are associated with the first (VA1) and second (VA2) volcanic events (Routhier et al. 1980); no massive sulphides or chert are known in relation to the third event (VA3).

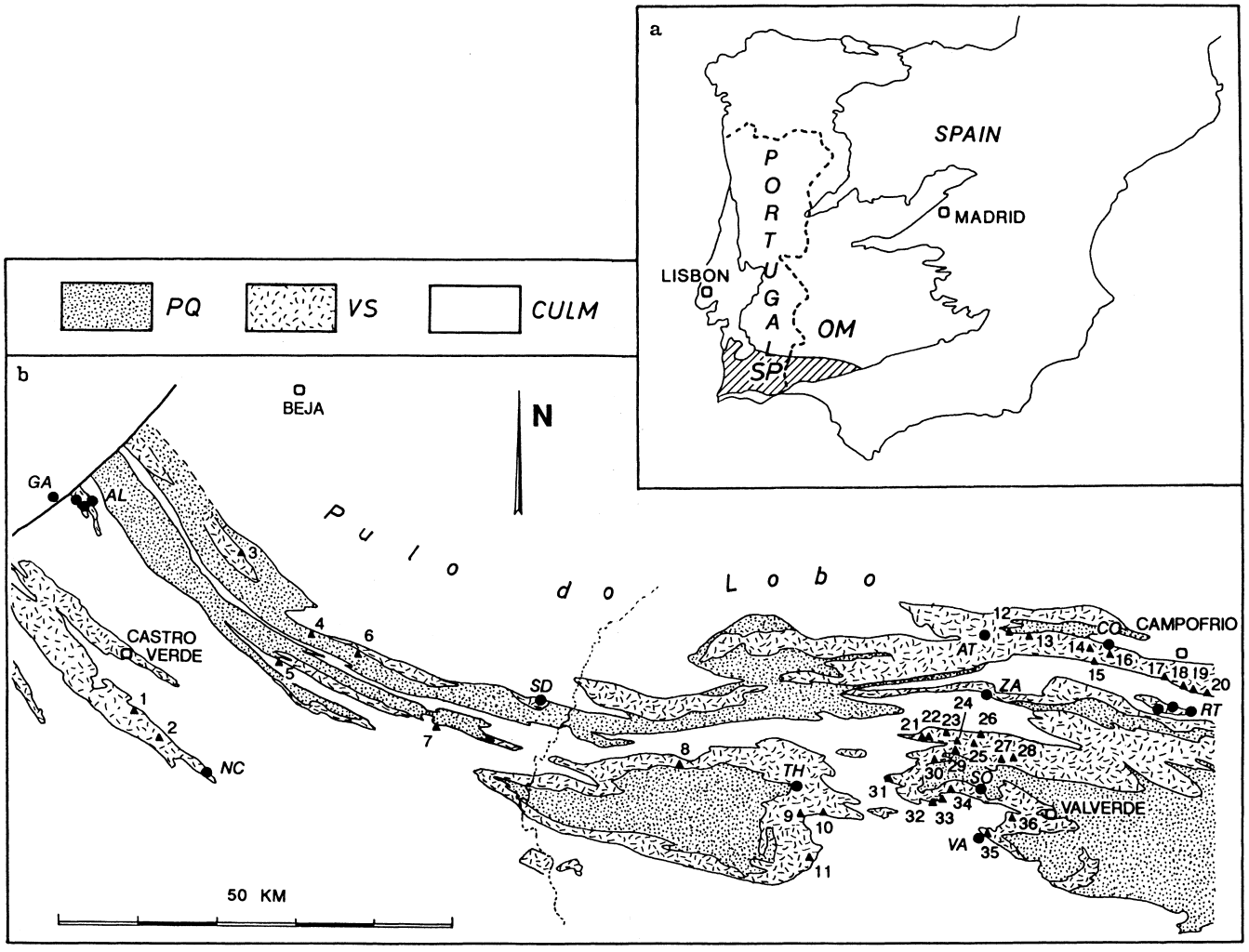

Fig. 1a Simplified geological map of the Iberian massif within the Iberian Hercynian belt (after Dallmeyer and Martínez García 1990). *SP*, South Portuguese Zone; *OM*, Ossa-Morena Zone **b** Simplified geological map of the study area showing the chert sample locations. *PQ*: phyllite and quartzite – Upper Devonian; *VS*: volcano-sedimentary succession – upper Famenian to upper Visean; *CULM*: greywacke, pelite and conglomerate – upper Visean to Westphalian. Main massive sulphide deposits: *GA*: Gaviaõ; *AL*: Aljustrel (Moinho to the NW, Feitais to the NE; Algares to the S); *NC*: Neves-Corvo; *SD*: Saõ Domingos; *TH*: Tharsis; *VA*: Masa Valverde; *SO*: Sotiel-Migollas; *ZA*: La Zarza; *AT*: Aguas Teñidas; *CO*: Concepción; *RT*: Rio Tinto (Corta Atalaya to the W, Cerro Colorado in the centre, Planes-San Antonio to the E). Chert occurrences and associated facies studied in this work: *1*: Ferragudo; *2*: Serpa; *3*: Chaparro dos Amoladeiros; *4*: Mina Balanca; *5*: Courelas das Casas Novas; *6*: Alcaria Ruiva; *7*: Mértola; *8*: Vallejin; *9*: Colada; *10*: Chaparral; *11*: Los Guijos; *12*: Cueva de la Mora; *13*: Romerita-Angelita; *14*: Angostura; *15*: Soloviejo; *16*: San Platón; *17*: Campofrío; *18*: Porto Alegre; *19*: Los Ermitanos-Peña de Hierro; *20*: Mina Pepito; *21*: Pancho; *22*: Santiago; *23*: San José; *24*: Peña Gordo; *25*: Morante; *26*: Cerca del Pino; *27*: Rio Odiel-La Morita; *28*: Tinto Santa Rosa: *29*: Pozo Blanco-Rabaldea-Camacho; *30*: La Novia; *31*: La Fé; *32*: Adolfina; *33*: Nuestra Señora del Pilar; *34*: La Torerera; *35*: Los Mellizos; *36*: El Cuervo

This region, in which mining dates back to Antiquity, is one of the largest massive-sulphide provinces in the world, with more than 1700 Mt of sulphides (Leistel et al. 1997). Abundant small mines also worked the chert for its manganese content (more than 200 sites are known). Today only a few mines work the massive sulphides (Rio Tinto, Aznalcóllar, Sotiel, Neves-Corvo), whereas manganese mining has been totally abandoned. For more detail on the mineralization and its geological context the reader is referred to several published reviews (Pinedo Vara 1963; Carvalho et al. 1976; Strauss and Madel 1974; Routhier et al. 1980; Barriga 1990; Sáez and Almodóvar 1993; Leistel et al. 1994) and to this volume.

Previous work on the South Iberian chert, position in relation to the massive sulphides

The close relationship between the sulphide mineralization and certain layers of manganiferous chert was pointed out by Strauss (1970), who also reported the presence of radiolarites. The lithostratigraphic position of the chert with respect to the massive sulphides is commonly difficult to establish. Chert is present in the hanging wall rocks of some of the largest orebodies of the Province, in places being in direct contact with the sulphides or, more commonly, intercalated within the volcano-sedimentary rocks. Strauss and Madel (1974) and Strauss and Beck (1990) provide evidence for the Lousal, La Zarza and Tharsis deposits. At Lousal, the miner-

alization is hosted by a pelitic sequence and chert is only seen higher in the succession. At La Zarza the epiclastite and tuffite of the hanging wall contain many chert lenses, most of which are several tens of metres above the sulphides; locally, however, some lenses are in direct contact with the mineralization. Chert is also present in the calcareous shale of the hanging wall at Tharsis, but not in direct contact with the massive sulphides. At Rio Tinto red hematitic chert is associated with the sulphides of the Planes San Antonio orebody; it is represented as being in a lateral position relative to the feeder stockwork and lying directly on the sulphide mass (Garcia Palomero 1990). The sulphides at Neves are capped by a pyritic blue chert and those at Corvo by an ankeritic bed (Leca et al. 1985). Barriga and Fyfe (1988) interpret the chert layer over the Feitais orebody (Aljustrel, Portugal) as being early and as having acted as a protective insulating cap favouring the precipitation of the sulphides; chert clasts are seen to be caught up within and wrapped around by the sulphides.

Relatively high Au contents (up to 1 ppm) and the existence of an As-Ni-Co-Ba-Sr-Li geochemical signatures in cherts are reported by Rahders and Germann (1993). Oxygen (Munhá et al. 1986) and sulphur (Routhier et al. 1980) isotopic analyses have provided indications about the hydrothermal fluids and the origin of the sulphur contained in the chert. Finally, geochemical studies of the chert, both associated with and unassociated with the sulphides, were carried out by Barriga and Oliveira (1986) and Barriga (1986, 1990), who concluded that the chert was formed through chemical precipitation from hydrothermal fluids composed mainly of sea water at stratigraphic intervals that were not necessarily related to the massive sulphides. For these authors, the criteria for an association of chert with a nearby mineralization would be: (1) the reduction of the hematitic chert to pyritic chert; (2) the presence of veins, pockets and breccias with manganiferous minerals; (3) a negative Ce anomaly; (4) low Co, Ni, Cu, Zn and Pb contents in relation to Fe and Mn; (5) a positive Au anomaly; and (6) an absence of radiolarians.

Sampling and analytical methods

Fifty four outcrops of chert and associated facies were examined in the field in both Spain and Portugal. Their position in the lithostratigraphic column and their possible relationship with a massive sulphide type mineralization were systematically looked for. Forty samples were analyzed; 28 by ICP-MS (major, trace and rare earth elements) and atomic absorption (Au) and 12 by ICP (major and trace elements) and atomic absorption (Au). Twenty four chert samples were analyzed for their lead isotopes, and the results corrected for radiogenic enrichment by taking the age t = 351 Ma, which is the average age of the volcano-sedimentary succession; five of these were discarded due to high values of their μ ratio ($^{238}U/^{204}Pb$) which penalises the precision of the corrections. The rare earth diagrams were chondrite normalized using the values of Boynton (in Henderson 1984). The Ce anomalies were calculated by the following formula (as was Eu by replacing La and Pr by Sm and Gd):

$$\frac{Ce}{Ce*} = \frac{Ce_N}{\sqrt[2]{La_N * Pr_N}} \qquad \frac{Ce}{Ce*} = \frac{Ce_N}{\sqrt[3]{(La_N)^2 * Nd_N}}$$

(N means chondrite normalized)

Macroscopic and microscopic description of the chert and associated facies

Occurrence and distribution

The chert is either pale grey-white to greenish or dark red in colour, with a massive or thinly bedded appearance. It occurs in stratiform lenticular beds, from a centimetre to several decimetres thick and from a decametre to several hundred metres long, that are resistant to weathering and thus commonly form crests and ridges in the landscape. Massive manganese silicate and carbonate layers are in places associated with the chert, but are much less common. The contacts with the volcano-sedimentary country rock are generally very sharp. Mapping difficulties (condensed sequences, lateral facies variations, major tectonic complications) commonly result in an uncertainty as to the position of the chert (observed in outcrop) within the volcano-sedimentary succession, but schematically it is localized at two main levels (Fig. 2).

In the lower level, the chert occurs either directly at the top of the lower acidic volcanites and associated basic volcanites of VA1, or a few metres higher in the tuffite, pelite and black schist. This lower level is generally considered as the main host of the sulphide mineralization, but nowhere in the field have we observed a lateral passage from chert to sulphide. Places where the chert is very close to the sulphides are Fetais (Aljustrel), Vallejin (Herrerías); at the top of the Corvo orebody we were able to sample the decimetre-thick ankeritic layer. The chert of the lower level is in places seen as reworked pebbles in the tuffaceous and epiclastic beds at the base of the overlying VA2.

In the upper level, the chert occurs within the VA2 acidic volcanites and pyroclastites, in places fairly low in the succession, a few metres above the massive sulphides overlying VA1 facies, and in places very high and close to the marker bed of purple schist, if not directly in contact with it. It is likely that the chert of the upper level is not everywhere at a strictly equivalent stratigraphic level. It can also be seen as reworked clasts in the overlying beds.

From the distribution of the four types of chert and associated facies we describe (see below), no specific regional distribution and no special link with the massive sulphides can be established.

Petrography and mineralogy

Four main types of chert and associated facies have been mapped:

Red hematitic chert ± magnetite

Red hematitic chert ± magnetite, which is easily distinguished by its red colour (Plate IA), is widespread

►

Fig. 2 Schematic lithostratigraphic logs showing the chert sample locations (vertical scale indicative). *1*: pelite and greywacke – Culm; *2 to 16*: volcano-sedimentary succession; *2*: tuffite, ignimbrite (VA3); *3*: purple schist; *4*: chert; *5*: conglomeratic chert; *6*: pyritic chert; *7*: gabbro-dolerite; *8*: basalt; *9*: fine-grained pelite-cinerite-tuffite; *10*: tuff; *11*: rhyolite; *12*: pyroclastite (with chert and pelite elements); *13*: porphyritic rhyodacite; *14*: pyroclastite with blocks; *15*: massive sulphides; *16*: stockwork; 17: phyllite and quartzite – Devonian

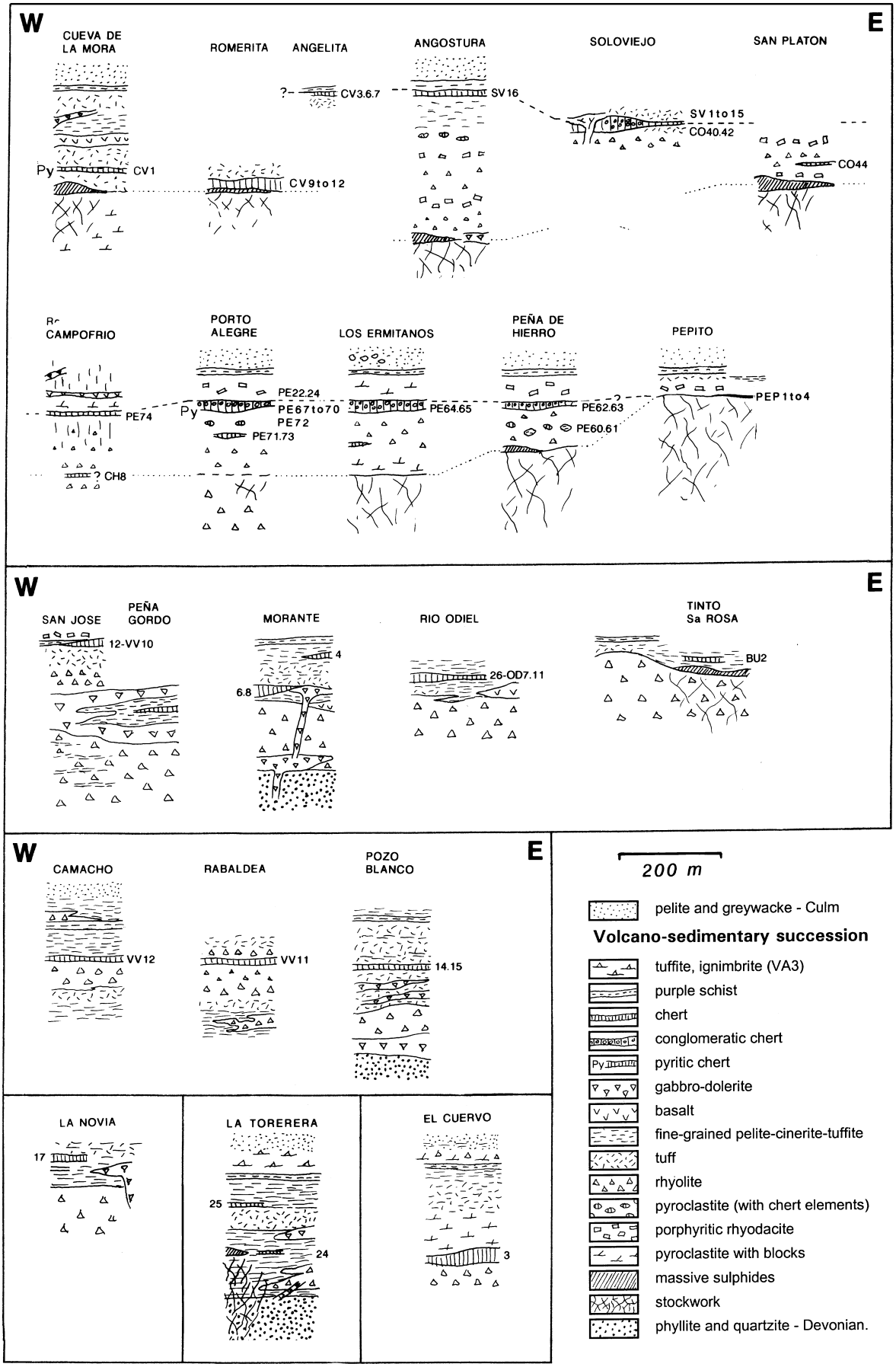
W
E
CUEVA DE LA MORA
ROMERITA
ANGELITA
ANGOSTURA
SOLOVIEJO
SAN PLATON
Py
CV1
CV9to12
?
CV3.6.7
SV16
SV1to15
CO40.42
CO44
CAMPOFRIO
PORTO ALEGRE
LOS ERMITANOS
PEÑA DE HIERRO
PEPITO
PE74
? CH8
PE22.24
PE67to70
PE72
PE71.73
PE64.65
PE62.63
PE60.61
PEP1to4
SAN JOSE
PEÑA GORDO
MORANTE
RIO ODIEL
TINTO Sa ROSA
12-VV10
4
6.8
26-OD7.11
BU2
CAMACHO
RABALDEA
POZO BLANCO
VV12
VV11
14.15
LA NOVIA
17
LA TORERERA
25
24
EL CUERVO
3
200 m
pelite and greywacke - Culm
Volcano-sedimentary succession
tuffite, ignimbrite (VA3)
purple schist
chert
conglomeratic chert
pyritic chert
gabbro-dolerite
basalt
fine-grained pelite-cinerite-tuffite
tuff
rhyolite
pyroclastite (with chert elements)
porphyritic rhyodacite
pyroclastite with blocks
massive sulphides
stockwork
phyllite and quartzite - Devonian.

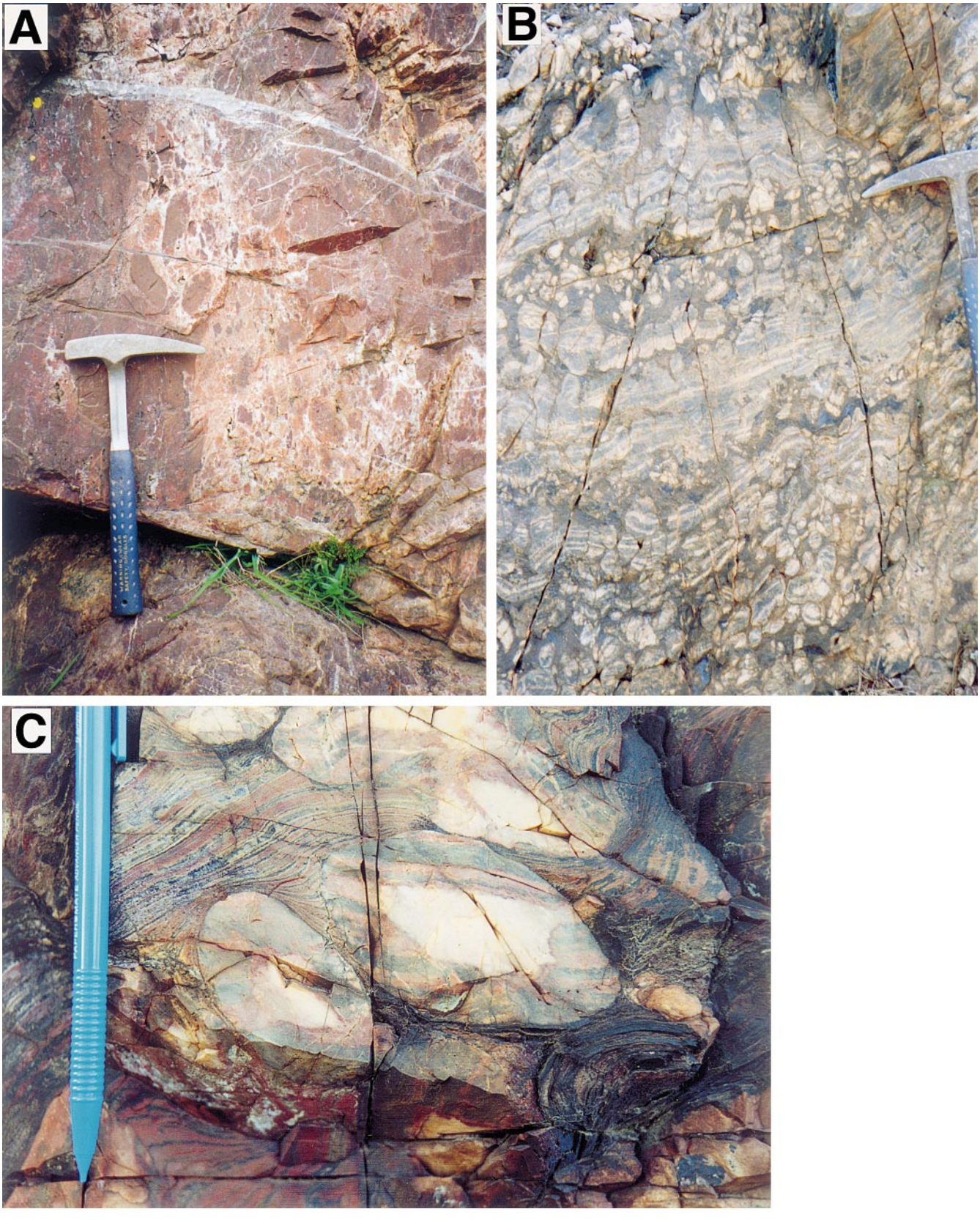
A
B
C

throughout the Province in both the lower and upper levels of the succession. In places it is seen to have developed at the expense of the volcanic or sedimentary host rock and is locally reworked as pebbles in the overlying tuffaceous and epiclastic beds; its genesis appears to be very early (pre- to syn-diagenetic) and to have taken place in the immediate environment of the water/sediment-pyroclastite interface.

Silica, as microcrystalline quartz, is largely predominant. Hematite, finely crystalline, is abundant and is commonly associated with magnetite resulting from a phase of muschketovitization (alteration of hematite to magnetite). At least two stages of silica + hematite are seen, the second microbrecciating the first and also being richer in hematite. Clast-matrix contacts are irregular and commonly diffuse, such as would be formed by a percolation of more ferriferous fluids through an unconsolidated facies.

The clasts commonly have a submillimetric spherulitic structure imparted by a fibroradial silica crystallization (chalcedony) dotted with hematite, in places with a quartz grain nucleus (Plate IIA). The composition of the spherulites appears to be very homogeneous under the SEM; only silica with the internal structure being marked by variations in colour, probably due to very weak traces of iron oxide, and possibly also containing small inclusions of phengite. Certain spherulite masses show fine cracks invaded by pale microcrystalline quartz and reminiscent of desiccation cracks. Such siliceous spherulites can form through the crystallization of chalcedony from colloidal siliceous gels (Oehler 1976).

The magnetite of the chert is euhedral and poikiloblastic, forming strings of submillimetre-size aggregates and also very small (5 μm) disseminated crystals. Chlorite may be associated; it is very ferriferous with low concentrations of Mn and Mg. The magnetite ± chlorite phase is everywhere later than the hematite, which it pseudomorphoses. Microcrystalline calcite (with weak traces of Fe, Mn and Mg) forms nebulous submillimetre-size spots in the siliceous matrix.

Sulphides are nowhere abundant and their paragenetic position is variable; they are generally later than the oxides and appear to be associated with patches of carbonate. They consist mainly of millimetre-size euhedral pyrite, in places with inclusions of pyrrhotite-chalcopyrite, much more rarely of galena and exceptionally of cobaltite associated with the magnetite (Los Guijos). The chronological position of these sulphides is difficult to determine; they may have developed due to diagenesis, or much later during late- or post-Hercynian deformation.

◄

Plate IA–C Photographs of South Iberian chert exposures. **A** Los Enjambres (between Angostura and Concepción): red hematitic chert cut and brecciated by the pale silica, and later intersected by subhorizontal veins of white quartz. **B** Los Ermitanos: conglomeratic chert from the Soloviejo-Porto Alegre level; the pale siliceous layers break down to form conglomeratic intervals. **C** Detail of B: the clasts show a core of white silica and a layering identical to that in the matrix except that it is not compacted, which indicates very early silicification

Radiolarian chert and conglomeratic chert

The radiolarian chert and conglomeratic chert are lateral or vertical facies variations of the red hematitic chert ± magnetite. In Spain, they are seen only in the upper level. In Portugal, however, in the Monte Forno da Cal area (near Neves-Corvo), a bedded radiolarian chert facies is associated with grey chert at the top of porphyritic acidic volcanites considered as VA1 and below black schist. However, the VA2 acidic volcanites are absent in this region (Leca et al. 1983) and so direct comparison with the Spanish part is impossible.

Radiolarians can be very abundant at some levels (Plate IIE, F); they are large (80 to 250 μm) and commonly visible macroscopically. Extractions, through controlled attack with dilute hydrofluoric acid, yielded only bioclasts and incomplete radiolarian remains of spherical forms (*Spumellaria*), with the spongy test of the family *Entactiniidae*; this family was well developed through Ordovician to Carboniferous ages (determination by Ch. Bourdillon, BRGM, written communication). Radiolarians from phosphate nodules in the tuff of the Lousal area (Portugal) have been compared to species of the *Spumellaria* superfamily *Liosphaeracea*, with several forms resembling *Hexastylus dimensivus* Haeckel (Strauss 1970). An SEM examination of the radiolarian structure shows that it is made up of very fine quartz crystals (<10 μm) and thus can be completely camouflaged by the siliceous matrix.

The conglomeratic chert is known only from the Soloviejo-Porto Alegre level (Figs. 1, 2). Overlying a basal bed of massive hematitic radiolarian chert, less than 1 m thick, a bedded chert facies becomes progressively more reworked upwards to form balls or pebbles within a black, very manganiferous, varved matrix containing abundant radiolarians (Plate IB). The pebbles commonly show a silicified core of white quartz and a bedding similar to that of the matrix, but without compaction or flattening (Plate IC). It would appear that this structure results from the erosion of a partly silicified and early indurated layer in an unconsolidated mud. Various phenomena may have had an influence in the formation of this facies: gravity slides, density differences and "immiscibility" between the silica gel and the mud.

Pale (white, grey or grey-green) sulphidic chert

Pale sulphidic chert is very widespread. It cuts the hematitic chert more or less abundantly as puffs, veinlets and veins (Plates IA, IIG and IIB), and it commonly comprises the entire outcropping facies. It is formed of microcrystalline quartz (<100 μm) that developed in

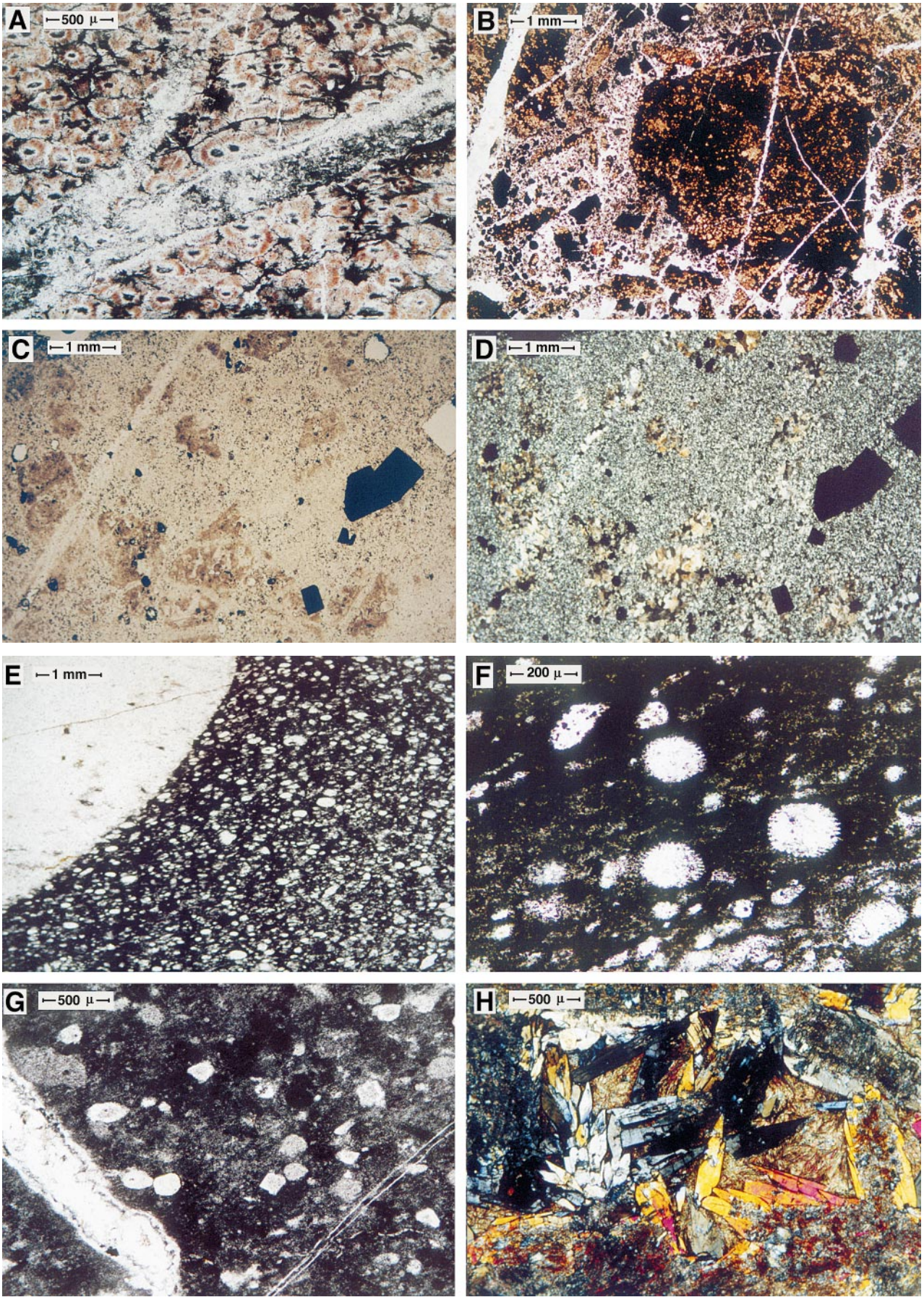
A
500 µ
B
1 mm
C
1 mm
D
1 mm
E
1 mm
F
200 µ
G
500 µ
H
500 µ

two main phases and which contains almost the totality of the sulphides. The first phase is represented by "large" quartz crystals (50 to 100 μm) with common inclusions of hematite grains and needles that give it a "dirty" appearance in thin section and a somewhat "marbled" macroscopic appearance. The second phase is a fairly diffuse network of paler (white to light grey) microcrystalline quartz (with few or no inclusions) developed at the expense of, or through brecciation of, the first phase quartz (Plate IIC, D). The sulphide paragenesis is polymetallic with dominant pyrite, marcasite, destabilized pyrrhotite, chalcopyrite, sphalerite (without cassiterite), galena and arsenopyrite, commonly associated with granules of carbonate or, more rarely, chlorite. The carbonates have an intermediate composition between siderite and rhodochrosite; the chlorite is everywhere very ferriferous, with traces of Mn and Mg. Veinlets and veins, reminiscent of tension gashes and containing large crystals of pale quartz without sulphides, cut the micro-crystalline quartz.

Rhodonite and/Mn carbonate ± magnetite facies

Fe carbonates (siderite, ankerite) or Mn carbonates (Mg-kutnahorite, rhodochrosite) and rhodonite are relatively common minerals in the veins cutting the siliceous chert facies. They locally form massive layers which were mined for their manganese. Although the relationships between the siliceous and the carbonate-silicate facies were not observed in the field, the microscopic relationships indicate that the rhodonite-carbonate facies are relatively younger.

The hematitic or siliceous chert is thus commonly cut by quartz + carbonate + pyrite ± chlorite and chlorite + pyrite veinlets. The siliceous groundmass of the bedded facies and the radiolarian chert generally contains submillimetre-size patches of carbonate or rhodonite and, more rarely, is cut by veinlets and layers of quartz + Mn-phlogopite (manganophyllite) ± rhodonite ± Mn-garnet (spessartine with traces of Ca) and Ba-rich potassium feldspar.

In the samples of apparently massive carbonate (phase between siderite and rhodochrosite), the carbonate appears to form either a very dense network of veinlets with dominant carbonate + quartz ± chlorite, which envelopes relict patches of pale microcrystalline quartz, or diffuse puffs replacing a red hematitic chert whilst retaining the original spherulitic texture. Sulphides (pyrite) are everywhere intimately associated with the carbonate. The massive rhodonite facies comprises millimetre-size aggregates of rhodonite with, at the edge, a radial crystallization (locally vuggy) of limpid rhodonite crystals; the interstices are filled with carbonate (slightly calcic rhodochrosite) and an indeterminate Mn silicate containing Cl (rhodonite?; Plate IIH).

The high mobility of manganese during weathering makes it difficult to identify the primary host minerals and their characters in the early stages of hydrothermal alteration. Moreover, weathering may have occurred at any stage from diagenesis to the present day. The red hematitic chert and the pale sulphidic chert seem to be devoid of primary manganese outside of the carbonate-rhodonite veins; only supergene reconcentrations of Mn oxides and peroxides form in the abundant fractures, microfractures and pockets of these very competent layers. Other than the reconcentrations, the commonly radiolarian purplish-red bedded facies in places contains rhodonite and Mn carbonate, and more commonly Mn oxides that may be either primary or derived from Mn carbonate or silicate. These generally form amorphous wads associated with nsutite (γ-Mn[O,OH]$_2$) and ramsdellite (γ-MnO_2) (X-ray determination).

The greenschist-type regional metamorphism and deformation related to the Hercynian orogeny caused recrystallization of the primary phases, mainly silica but also in part hematite and sulphides. The most visible phenomena are the recrystallization of chalcedony to polygonized microcrystalline quartz and the muschketovitization of hematite with the magnetite oriented along the foliation plane of the rock. The paragenesis of manganophyllite, rhodonite and spessartine, observed in a single sample, could be of metamorphic origin, although these minerals are also known in hydrothermal deposits (Roy 1981). Finally, sulphide-free veins of white quartz cutting the different types of chert and associated facies, mark tension gashes probably related to the regional deformation.

To summarise, the chronological succession of the hydrothermal phases can be expressed as follows: (1) silica + hematite; (2) silica + sulphides; (3) carbonate and Mn silicate. Stages 1 and 3 correspond to oxidizing conditions of deposition, whereas stage 2 indicates reducing conditions. Stages 1 and 2 seems to register only a local evolution of the oxydizing-reducing conditions without no change in the fluid chemistry, when stage 3 marks the appearance of Mn and Ca. The deposition occurred close to the sea water – sea bed interface; the absence of well-defined stockwork-type feeder zones for

◄

Plate IIA–H Microphotographs (transmitted light) of the South Iberian chert and associated facies (*PPL*: plane-polarized light; *CPL*: crossed polarized light). **A** La Angelita: red hematitic chert with a quartz + hematite fibroradial spherulitic structure cut by quartz veinlets (number CV7, PPL). **B** Chaparro dos Amoladeiros: red hematitic chert cut and brecciated by a siliceous vein of limpid quartz (number XL11, PPL). **C-D** La Novia: grey pyritic (opaque crystals) chert reflecting three successive siliceous phases; *1*: coarse quartz clasts studded with hematite (dark under PPL), *2*: pale microcrystalline quartz groundmass, *3*: veinlet of pale coarse quartz (number 17b, C in PPL, D in CPL). **E** Soloviejo: chert with radiolarians (small pale ovoid clasts) and quartz pebbles (large pale clast) in a finely hematitic groundmass (number SV4, PPL). **F** Peña de Hierro: radiolarian chert; the structure of the radiolarians is clearly recognizable, the groundmass is finely hematitic (number PE63, PPL). **G** Embalse del Alisal: red hematitic chert cut by a vein of pale quartz; geometric ghosts of crystals can be recognized in the finely hematitic groundmass (number CV3, PPL). **H** Mértola: pink massive rhodonite; the groundmass and prismatic crystals are of rhodonite; the vugs are filled with carbonate (number XL15, CPL)

these deposits argues for a diffuse hydrothermal event probably with combined lateral migration, chemical precipitation and replacement. The main question that is raised by these observations is whether **the second hydrothermal event, with silica and sulphides, is related to the massive sulphide mineralization and whether it could represent an early aborted development towards this type of mineralization**. The adopted geochemical approach, which combines the use of trace elements, rare earth elements and lead isotopes, has provided a possible answer.

Chemical characteristics

The chert is obviously highly siliceous (SiO_2 commonly >90%), with facies that are rich in Mn (up to 44% MnO) or Fe (up to 36% Fe_2O_3 + FeO) and poor in Co + Ni + Cu (<400 ppm) (Fig. 3; Table 1). Two groups are distinguished:

a. A manganiferous group, which consists almost exclusively of samples from the Soloviejo and Santiago level, as well as a sample from the Pepito mine (Figs. 1, 2); but not all the samples from this level are manganiferous;
b. A ferriferous group, which includes all the other chert samples and notably most of the radiolarian chert; this group contains the highest Co + Ni + Cu content.

The Ti and Al contents of certain South Iberian samples are relatively high and, although no good correlation seems to exist, the increase in Ti is generally accompanied by an increase in Al. This tends to indicate the participation either of a detrital component or of relicts of the country rock in the composition of the chert. The contamination curve of the chert shows a trend towards a pole corresponding to the composition of the South Iberian volcanites (Fig. 4), which thus appear to be a very likely source for the residual or detrital component. The contamination is well marked in certain radiolarian chert samples, where it is logical to see the trace of a sedimentary contribution, and also in facies where relicts and clasts of the country rock are visible under the microscope (Plate IIG). The latter facies also show an obvious trend towards an acidic volcanic pole in the Al versus. ΣREE diagram (Fig. 5). In a general way, it is also the contaminated facies that give the highest absolute rare-earth content; therefore it is necessary to eliminate the contaminated facies in order to study the rare earth signature of the chert. Through considering the chert in relation to its facies, we have been able to reveal the following chemical particularities.

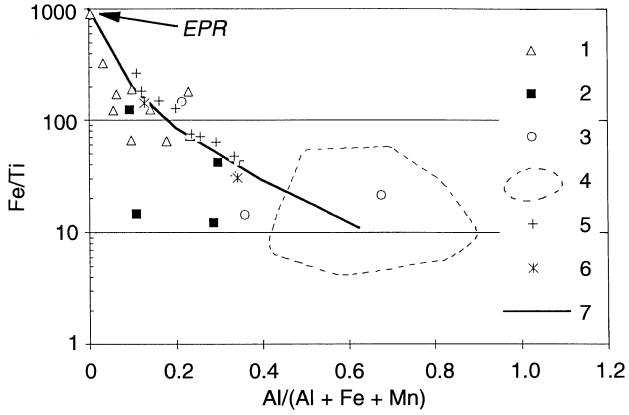

Fig. 4 Al/(Al + Fe + Mn) versus Fe/Ti plot of the South Iberian chert and volcanic rocks revealing the presence of a hydrothermal pole and a volcano-sedimentary pole within the chert (diagram after Bostrom 1973; Wonder et al. 1988; composition of the South Iberian volcanites after Thiéblemont et al. 1994). *1*: chert; *2*: radiolarian chert; *3*: contaminated chert; *4*: volcanite field; *5*: Key Tuffite; *6*: Tetsusekiei; *7*: mixing curve between hydrothermal sediments of the East Pacific Rise (EPR) and pelagic terrigenous sediments

Geochemical signature of the radiolarian chert

The radiolarian chert (a) can be fairly rich in Ba (80 to >3500 ppm), (b) can contain traces of Al (Al_2O_3 = 0.9

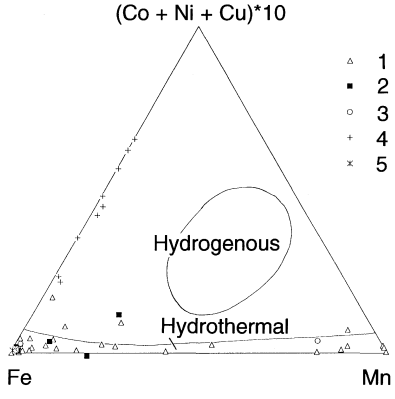

Fig. 3 Fe-Mn-(Co + Ni + Cu)*10 diagram revealing the hydrothermal character of the South Iberian chert (fields of hydrothermal deposition and "hydrogenous" deposition of the marine manganiferous deposits after Bonatti et al. 1972). *1*: chert; *2*: radiolarian chert; *3*: contaminated chert; *4*: Key Tuffite ; *5*: Tetsusekiei

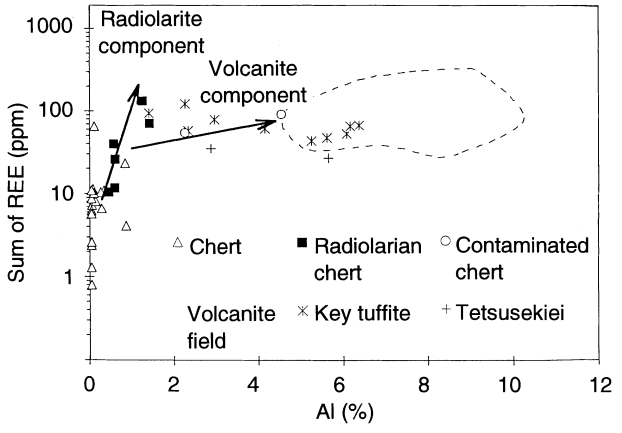

Fig. 5 Al versus ΣREE plot of the South Iberian chert and volcanites. *1*: chert; *2*: radiolarian chert; *3*: contaminated chert; *4*: volcanite field; *5*: Key Tuffite; *6*: Tetsusekiei

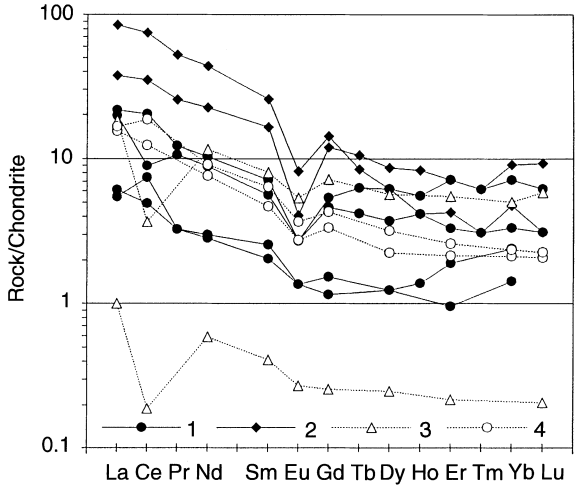

Fig. 6 Rare-earth plot of the South Iberian radiolarian chert and radiolarites. *1*: Soloviejo and Porto Alegre; *2*: Santiago and San José; *3*: Cenozoic radiolarian ooze from the Deep Sea Drilling Project (DSDP); *4*: Kamiasô Permian-Jurassic radiolarian chert (Gifu, Japan). (*3* and *4* after Shimizu and Masuda 1977)

to 3.8%), Ti and Rb, (c) are fairly hematitic with $Fe_2O_3 \leq 8.3\%$, (d) is also enriched in Th (>0.8 ppm), but (e) contains no FeO, CaO or Au. Only one sample (Santiago) was distinguished by its high Cu content.

The absolute ΣREE contents are clearly higher than those of chondrite (factor of 1 to 100; Fig. 6) and are high compared with the average contents of the other chert. A ΣREE trend is seen from the poorest facies in the Soloviejo level in the east to the richest facies at San José-Santiago in the west. This essentially reflects the higher light rare earth (LREE) content at San José-Santiago. Normalizing to chondrite shows a slight positive Ce anomaly (Ce/Ce* = 1.16 to 1.38 on the La-Nd curve), a negative Eu anomaly (Eu/Eu* = 0.29 to 0.79) and an enrichment in LREE.

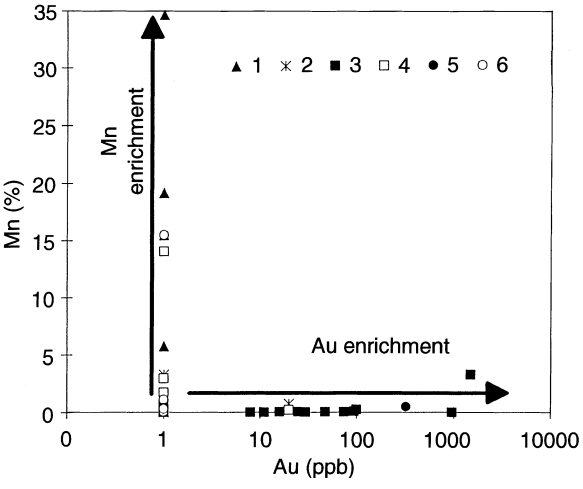

Fig. 7 Au versus Mn plot of the South Iberian chert (the auriferous facies contain the sulphides and show Mn depletion). *1*: Mn oxides and carbonates; *2*: contaminated chert; *3*: lower sulphide-bearing chert; *4*: lower oxide-bearing chert; *5*: upper sulphide-bearing chert; *6*: upper oxide-bearing chert

Geochemical signature of the other chert

The hematitic chert is generally richer in Fe than the sulphidic chert (Table 1). Au is everywhere associated with the pale siliceous facies with variably abundant sulphides and no Mn (Fig. 7). The highest observed Zn and Pb concentrations correspond to the sulphide facies, but the evolution of the oxide facies towards the sulphide facies is reflected mainly by an enrichment in Zn (Fig. 8) and an increase in the Au/Mn ratio (Fig. 8b). Pb is very variable and no significant variation in Cu was detected. Apparently no distinction is seen between the chert of the lower level and that of the upper level.

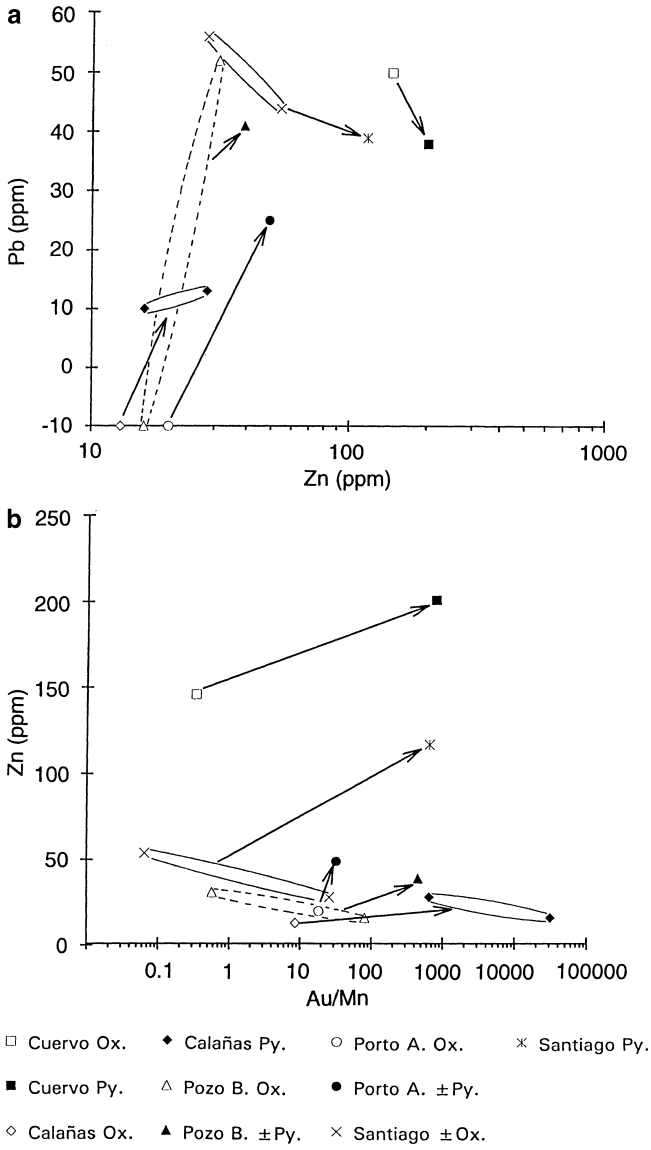

Fig. 8 a Zn versus Pb plot of specific chert beds to show the Zn enrichment when a sulphide facies affects an oxide facies. **b** Au/Mn versus Zn plot of specific chert beds showing the increase in the Au/Mn ratio and Zn concentration when a sulphide facies affects an oxide facies. (Chronology is known only between oxide and sulphide facies, but the sequence among sulphide or oxide facies is not determinable) *Ox.*: oxide-bearing chert; *Py.*: sulphide-bearing chert

The hematitic and sulphidic chert facies generally have lower rare earth contents (factor of 1 to 10 in relation to chondrite) than the radiolarites. The distinctions between "chert of the upper level – chert of the lower level" and between "hematitic chert – siliceous chert" alone do not reveal a fundamental difference, all being relatively homogeneous (Figs. 9, 10). The cerium anomalies are generally weak and seem to be indifferently positive or negative. The europium content is commonly lower than the analytical threshold of detection, which could confirm the weak negative anomalies noted in the few samples where this threshold is exceeded. Some chert shows a slight distinction in its attenuated V-shaped profile, which reflects an enrichment in heavy rare earths (HREE). This profile shape was found in three samples of hematitic chert (San Platón, Morante, Pepito) and two samples of sulphidic chert (Feitais, Morante) (Fig. 11a).

Lead isotopes

Lead isotope analysis shows that the isotopic signature of the chert is more radiogenic than that of the massive sulphide mineralization (Fig. 12): the $^{206}Pb/^{204}Pb$ ratios are between 18.20 and 18.44 for the chert (Table 2), against 18.13 to 18.23 for the massive sulphides (Marcoux et al. 1992, Marcoux 1997). Some hematitic and sulphidic chert shows signatures comparable to that of the massive sulphides, marking the end of a trend line towards the more radiogenic facies. The sulphide chert facies that are geometrically associated with the orebodies (Feitais, Vallejin) show isotopic signatures which are slightly to clearly more radiogenic than those of the massive sulphides ($^{206}Pb/^{204}Pb$ = 18.237 to 18.445). In addition, the sulphidic chert with the highest lead content (between 500 and 4000 ppm; Table 2) does not show a trend towards the massive-sulphide signature and remains more radiogenic: the sulphide enrichment

Table 1 Chemical analyses of chert. 1: sulphidic chert, lower level; 2: hematitic ± magnetite chert, lower level; 3: sulphidic chert, upper

	PF %	P_2O_5 %	SiO_2 %	Al_2O_3 %	Fe_2O_3 %	FeO %	CaO %	MgO %	Na_2O %	K_2O %	TiO_2 %	MnO %	Total major
AJ1	2.14	0.09	90.90	0.51	1.90	3.00	−0.10	−0.20	−0.20	−0.05	−0.05	0.07	98.01
8b	0.78	0.07	94.94	0.54	2.24	−0.20	0.11	0.25	−0.20	−0.05	−0.05	0.06	98.49
8d	0.20	0.08	90.90	−0.10	7.62	−0.20	0.23	−0.20	−0.20	0.05	−0.05	0.15	98.48
VV12	1.67	0.06	90.98	1.58	1.10	1.65	0.14	0.28	−0.20	0.43	−0.05	1.00	98.64
PE74	−0.10	−0.05	78.69	−0.10	21.10	−0.20	−0.10	−0.20	−0.20	−0.05	−0.05	0.07	98.81
4b	1.80	0.07	77.30	−0.10	20.68	−0.20	−0.10	−0.20	−0.20	−0.05	−0.05	0.08	99.03
CV3		0.05	84.70	−1.00	7.70	0.15	−1.00	−1.00		−0.50	0.02	1.49	90.61
CV1	1.26	0.07	79.82	8.58	1.14	1.60	0.17	0.33	2.41	3.29	0.16	0.04	98.87
3c	0.60	0.06	96.10	0.12	1.30	0.30	−0.10	−0.20	−0.20	0.12	−0.05	0.16	98.21
3e	1.65	0.09	89.50	0.28	3.90	−0.20	−0.10	−0.20	−0.20	0.17	−0.05	3.85	98.69
VL2		0.21	5.00	2.20	3.00	−0.05	−1.00	−1.00		0.80	0.02	20.00	29.18
17b		0.07	95.40	−1.00	3.20	1.35	−1.00	−1.00		−0.50	−0.01	0.07	96.58
VV11		0.06	63.20	6.90	18.80	0.18	−1.00	−1.00		1.10	0.15	0.13	88.52
PEP1	18.10	0.05	14.25	0.22	23.75	13.60	1.30	0.66	−0.20	−0.05	0.05	24.75	96.48
PEP3	11.65	−0.05	62.30	0.21	4.75	−0.20	1.40	0.30	−0.20	0.20	−0.05	18.15	98.46
6a	0.38	0.15	96.23	−0.10	2.27	−0.20	−0.10	−0.20	−0.20	−0.05	−0.05	0.04	98.17
25c	1.27	0.07	87.50	−0.10	8.95	0.65	−0.10	−0.20	−0.20	0.07	−0.05	0.44	98.30
25a	0.40	0.06	95.30	−0.10	1.95	0.47	−0.10	−0.20	−0.20	−0.05	−0.05	0.12	97.60
25a.bis		0.06	92.10	−1.00	4.40	2.00	−1.00	−1.00		−0.50	−0.01	0.80	95.85
26d	2.38	0.05	87.60	1.63	4.90	1.76	−0.10	0.20	−0.20	−0.05	−0.05	0.58	98.70
PE22		0.03	90.10	1.20	8.20		−1.00	−1.00		2.80	0.05	0.08	100.46
PE64	0.23	0.07	88.88	1.10	8.29	−0.20	−0.10	−0.20	−0.20	0.32	−0.05	0.14	98.28
PE62		0.04	33.20	1.60	−1.00	−0.05	1.20	−1.00		−0.50	−0.01	20.00	53.48
PE65		0.03	86.90	1.00	−1.00	−0.05	−1.00	−1.00		−0.50	0.04	7.40	91.72
PE69	0.72	0.07	92.00	1.16	4.40	0.36	−0.10	0.28	−0.20	−0.05	−0.05	0.04	98.63
PE68	0.20	0.06	90.60	0.88	6.59	−0.20	−0.10	0.22	−0.20	0.34	0.06	0.07	98.52
PE71	1.10	0.05	86.50	4.30	1.20	−0.20	0.93	0.67	−0.20	0.07	0.08	4.30	98.83
15a		0.14	75.00	−1.00	12.80	−0.05	−1.00	−1.00		−0.50	−0.01	4.30	88.48
14a	0.41	0.06	86.62	−0.10	9.35	1.50	−0.10	−0.20	−0.20	−0.05	−0.05	0.32	98.08
14d		0.07	87.80	−1.00	8.10	−0.05	−1.00	−1.00		−0.50	0.01	2.25	94.68
VV10	1.05	−0.05	89.40	2.69	4.05	0.22	−0.10	0.54	−0.20	0.53	0.12	0.39	98.64
CO44	−0.10	0.06	86.37	−0.10	13.55	−0.20	−0.10	−0.20	−0.20	−0.05	−0.05	0.05	99.03
12d.bis	2.83	0.06	88.00	0.65	1.55	3.70	1.01	0.38	−0.20	−0.05	−0.05	0.66	88.54
12d.ter		0.16	56.40	3.80	1.80	−0.05	1.00	−1.00		−0.50	0.14	20.00	81.75
12b	1.66	0.08	90.17	2.38	3.35	−0.20	−0.10	0.28	−0.20	0.29	0.30	1.00	99.01
SV4	0.28	0.09	94.00	1.14	2.47	−0.20	−0.10	−0.20	−0.20	0.32	−0.05	0.53	98.08
SV7	1.80	0.09	51.85	−0.10	0.26	−0.20	0.32	−0.20	−0.20	−0.05	−0.05	44.70	98.22
SV11		0.23	26.40	1.00	2.40	−0.05	−1.00	−1.00		1.00	−0.01	20.00	48.97
24a	1.92	0.09	87.00	0.16	6.95	2.44	−0.10	−0.20	−0.20	0.06	−0.05	0.04	98.11
VL1	0.36	0.17	96.50	−0.10	1.05	0.54	−0.10	−0.20	−0.20	−0.05	−0.05	0.05	97.97

(continued on p. 72)

of the chert does not therefore involve an enrichment in the massive-sulphide-type lead.

A common origin for the sulphides and associated manganese-iron oxides of present-day submarine hydrothermal mineralization (EPR near 7° N) is reflected in their similar lead isotopic compositions (Boulègue et al. 1984). As against this, the manganiferous encrustations intercalated in the oceanic crust basalt (EPR 21° N) show lead isotopic signatures very close to those of the marine sediments and are clearly more radiogenic than the sulphides of the hydrothermal vents; this tends to indicate that their source is the sea water (Brévart et al. 1981).

The lead contained in the chert would not therefore have exactly the same origin as that contained in the massive sulphides. The lead enrichment of the chert does not correspond to an evolution towards a massive sulphide type mineralization, but reflects the participation of another source. We seem here to be in an intermediate situation between the manganese-iron oxides and the manganiferous encrustations associated with present-day submarine hydrothermal sulphides. Thus a fairly significant participation of host sediments and/or sea water can be envisaged for the South Iberian chert. Radiogenic lead extracted from sediments rather than from sea water seems to account the relatively high lead content in chert; this has been proven in sedimented ridges such as Guayamas and Middle Valley (Shanks et al. 1995).

Significance and origin of the chert and associated facies – relationships with the massive sulphide mineralization

Comparison with reference models

The Key Tuffite and the Tetsusekiei are the reference models in the domain of exhalite layers associated with volcano-sedimentary massive sulphides, and their value

level; 4: hematitic ± magnetite chert, upper level; 5: radiolarite; 6: contaminated chert; 7: Mn oxides (−: below detection limit)

La ppm	Ce ppm	Pr ppm	Nd ppm	Sm ppm	Eu ppm	Gd ppm	Tb ppm	Dy ppm	Ho ppm	Er ppm	Tm ppm	Yb ppm	Lu ppm	Type	Location
1.6	2.5	0.3	1.6	0.4	−0.1	0.7	0.1	1.1	0.3	0.8	−0.1	0.9	0.1	1	Aljustrel
2.0	2.4	0.2	1.1	0.3	−0.1	−0.1	−0.1	0.2	−0.1	0.1	−0.1	0.3	−0.1	1	Calañas
1.2	1.1	0.2	1.2	0.5	−0.1	0.3	−0.1	0.6	0.1	0.4	−0.1	0.6	−0.1	2	Calañas
3.9	8.9	0.9	3.8	1.1	0.2	1.0	0.2	1.3	0.3	0.8	0.1	0.7	0.1	1	Calañas SW
0.4	0.5	−0.1	0.3	−0.1	−0.1	−0.1	−0.1	0.1	−0.1	−0.1	−0.1	−0.1	−0.1	2	Campofrio road
0.2	−0.1	−0.1	0.3	−0.1	−0.1	−0.1	−0.1	0.1	−0.1	−0.1	−0.1	0.2	−0.1	4	Cerca del Pino
−20.0	−10.0													4	Cueva Mora
15.9	34.7	4.0	16.7	3.4	0.3	3.4	0.6	4.7	1.0	3.1	0.4	3.2	0.4	6	Cueva Mora
1.4	2.6	0.2	1.3	0.3	−0.1	0.3	−0.1	0.6	−0.1	0.3	−0.1	0.2	−0.1	1	El Cuervo
1.2	2.7	0.2	1.5	0.5	−0.1	0.6	−0.1	0.6	0.1	0.3	−0.1	0.4	−0.1	2	El Cuervo
44.0	−10.0													7	Herrerias
−20.0	−10.0													1	La Novia
41.0	51.0													6	La Rabaldea
13.2	17.6	2.6	10.9	3.7	0.4	5.4	0.9	6.0	0.9	2.2	0.2	1.3	0.1	1	Mina Pepita
2.5	3.1	0.3	2.0	0.4	−0.1	0.4	−0.1	0.6	0.2	0.3	−0.1	0.4	−0.1	2	Mina Pepita
0.5	0.5	−0.1	0.3	−0.1	−0.1	−0.1	−0.1	−0.1	−0.1	−0.1	−0.1	−0.1	−0.1	2	Morante
0.5	0.9	−0.1	0.7	−0.1	−0.1	0.1	−0.1	0.2	−0.1	0.1	−0.1	0.1	−0.1	3	Na Sa Pilar
0.4	0.3	−0.1	0.4	0.1	−0.1	−0.1	−0.1	0.1	−0.1	−0.1	−0.1	−0.1	−0.1	4	Na Sa Pilar
−20.0	−10.0													4	Na Sa Pilar
0.8	1.3	0.2	0.9	0.2	−0.1	0.2	−0.1	0.2	−0.1	0.2	−0.1	0.1	−0.1	1	Odiel
−20.0	−10.0													2	Peña de Hierro
6.7	16.3	1.5	6.2	1.4	0.2	1.4	0.3	2.0	0.4	1.5	0.2	1.5	0.2	4	Peña de Hierro
−20.0	18.0													7	Peña de Hierro
−20.0	−10.0													7	Peña de Hierro
6.1	7.2	1.3	6.3	1.1	0.2	1.2	0.2	1.2	0.3	0.7	0.1	0.7	0.1	4	Porto Alegre
1.9	4.0	0.4	1.8	0.5	0.1	0.3	−0.1	0.4	0.1	0.4	−0.1	0.5	−0.1	4	Porto Alegre
11.1	24.0	2.6	9.2	2.0	0.2	1.4	0.2	1.4	0.3	0.8	−0.1	0.9	0.1	6	Porto Alegre
−20.0	−10.0													2	Pozo Blanco
0.6	0.8	0.1	0.5	0.1	−0.1	−0.1	−0.1	0.2	−0.1	−0.1	−0.1	0.1	−0.1	2	Pozo blanco
−20.0	−10.0													2	Pozo Blanco
11.6	28.3	3.1	13.4	3.2	0.3	3.1	0.5	2.8	0.6	1.5	0.2	1.9	0.3	4	San José
1.2	2.5	0.2	1.0	0.2	−0.1	0.2	−0.1	0.6	0.2	0.7	0.1	1.5	0.3	2	San Platón
2.0	4.4	0.4	2.1	0.4	0.1	0.4	−0.1	0.6	−0.1	0.2	−0.1	0.3	−0.1	3	Santiago
−20.0	−10.0													5	Santiago
26.4	60.2	6.4	26.1	5.0	0.5	3.7	0.4	2.0	0.3	0.9	0.1	1.0	0.1	5	Santiago
1.7	6.0	0.4	1.7	0.4	0.1	0.4	−0.1	0.4	−0.1	0.2	−0.1	0.3	−0.1	4	Soloviejo
2.7	1.6	0.5	2.5	0.5	0.1	0.8	0.1	0.8	0.2	0.5	−0.1	0.6	−0.1	7	Soloviejo
28.0	64.0													7	Soloviejo
3.4	4.3	0.4	1.9	0.4	−0.1	0.3	−0.1	0.4	−0.1	0.2	−0.1	0.1	−0.1	1	Torerera
2.1	1.4	0.3	1.4	0.2	−0.1	−0.1	−0.1	0.2	−0.1	0.1	−0.1	−0.1	−0.1	1	Vallejin

(continued on p. 73)

Table 1 (continued)

	Y ppm	Zr ppm	Nb ppm	Hf ppm	Th ppm	Ta ppm	U ppm	Rb ppm	Ni ppm	Cr ppm	V ppm	Sr ppm	Ba ppm	Co ppm
AJ1	4.4	2	0.1	−0.1	0.1	0.2	0.9	−1	30	30	65	86	18	9
8b	1.3	3	0.3	−0.1	0.3	−0.1	1.2	1	197	21	16	−5	−10	84
8d	3.2	4	0.3	−0.1	−0.1	−0.1	0.9	2	23	25	19	−5	−10	−5
VV12	7.5	21	1.2	0.4	1.6	0.1	1.2	18	25	18	16	−5	97	9
PE74	1.4	−1	−0.1	−0.1	−0.1	−0.1	0.3	−1	15	−10	10	−5	10	−5
4b	1.2	−1	−0.1	−0.1	−0.1	−0.1	1.9	−1	21	16	27	−5	32	−5
CV3	−20.0	110	−20						29	19	76	31	113	6
CV1	23.4	94	4.6	2.5	7.2	0.5	1.7	44	19	20	12	23	376	7
3c	5.1	3	0.7	−0.1	0.2	−0.1	0.6	5	27	33	28	−5	12	−5
3c	5.9	2	0.2	−0.1	0.2	−0.1	3.1	3	36	18	24	18	128	6
VL2	32.0	144	44						82	20	−10	924	168	64
17b	−20.0	191	−20						28	16	−10	14	−10	5
VV11	26.0	231	−20						41	−10	67	137	277	10
PEP1	38.1	2	0.5	−0.1	0.2	−0.1	1.8	−1	34	−10	42	30	112	10
PEP3	6.9	3	0.5	−0.1	0.3	−0.1	0.3	5	26	−10	10	32	196	10
6a	0.7	2	−0.1	−0.1	−0.1	−0.1	0.2	−1	15	16	16	−5	−10	−5
25c	1.8	−1	−0.1	−0.1	−0.1	−0.1	0.2	1	31	16	−10	5	42	6
25a	1.1	2	−0.1	−0.1	−0.1	−0.1	0.4	−1	28	19	17	−5	−10	−5
25a.bis	−20.0	88	−20						58	29	14	13	−10	5
26d	1.7	3	0.3	−0.1	−0.1	−0.1	0.5	−1	29	15	20	−5	−10	6
PE22	−20.0	134	−20						23	38	38	8	179	−5
PE64	11.2	10	1.2	0.2	0.8	0.1	0.9	15	19	14	16	13	874	5
PE62	−20.0	110	32						52	−10	−10	120	3500	58
PE65	−20.0	262	−20						36	−10	16	294	3500	10
PE69	6.4	8	0.9	0.2	0.9	−0.1	0.6	1	32	21	25	7	91	6
PE68	3.3	9	1.0	0.2	1.0	0.1	1.1	14	22	19	34	−5	169	6
PE71	6.9	18	2.0	0.6	1.5	0.2	2.4	1	23	16	10	125	43	7
15a	−20.0	43	−20						73	19	28	94	12	27
14a	1.8	2	0.3	−0.1	0.2	−0.1	0.7	−1	42	33	21	7	−10	8
14d	−20.0	99	−20						46	14	−10	65	34	6
VV10	13.3	26	3.9	0.6	1.8	0.2	0.8	26	63	22	147	15	209	11
CO44	5.0	12	0.1	0.2	0.2	−0.1	1.0	−1	15	−10	23	−5	−10	−5
12d.bis	3.5	3	0.3	−0.1	0.3	−0.1	0.5	1	23	18	12	−5	−10	14
12d.ter	−20.0	386	24						96	38	18	212	3500	70
12b	6.9	54	8.9	1.1	5.2	0.4	1.9	10	50	39	35	6	86	18
SV4	2.5	9	0.9	0.2	0.8	0.1	0.3	15	−10	13	12	29	446	−5
SV7	12.4	2	0.9	−0.1	0.2	−0.1	6.2	−1	68	16	14	128	158	16
SV11	48.0	116	32						36	−10	22	1252	3500	162
24a	2.2	3	0.3	−0.1	0.3	−0.1	0.1	−1	27	19	16	30	37	5
VL1	1.2	3	0.3	−0.1	0.2	−0.1	0.4	−1	23	27	24	6	−10	−5

in mineral exploration has already been emphasized (Scott et al. 1983).

Key Tuffite (*Matagami district*, *Archean Abitibi greenstone belt*, *Canada*)

The Key Tuffite is a continuous marker horizon, less than 6 m thick, that overlies or grades laterally into the massive sulphide orebodies and which separates the Watson Lake Group with its tholeiitic rocks (below) from the Wabassee Group with its calc-alkaline rocks (above) (Roberts 1975). It comprises fragments of tuff and chert-type exhalative sediments, along with disseminated and massive sulphides, and carbonates. The Key Tuffite facies is divided into two groups on the basis of its Zr/Y and La_N/Yb_N ratios; one assigned to the tholeiitic type and the other to the calc-alkaline type. The lower and upper levels therefore both participated in the tuffitic component of the Key Tuffite (Liaghat and MacLean 1992). The average grades of the Key Tuffite are 1.4% Zn, 0.1% Cu, with anomalies in Pb, Co, Ni, Cr; a richness in chert and carbonates, an increases in Cu, Zn and other base metals, and a thickening of the bed are associated with the proximity of the massive sulphide bodies (Davidson 1977). Liaghat and MacLean (1992) consider that the formation of the Key Tuffite horizon would have been identical to that described for present-day hydrothermal mineralization at the mid-ocean ridges.

Tetsusekiei (*Kuroko*, *Hokuroku district*, *Miocene*, *Japan*)

The Kuroko-related exhalites with a tuffaceous or tetsusekiei component (Kalogeropoulos and Scott 1983) occur most commonly as a discontinuous horizontal stratiform layer, less than 30 cm thick and with a lateral extension as much as twice that of a massive orebody,

Li ppm	Be ppm	B ppm	Cu ppm	Zn ppm	As ppm	Mo ppm	Ag ppm	Cd ppm	Sn ppm	Sb ppm	W ppm	Pb ppm	Bi ppm	Au ppb
−10			65	29	224	5	−0.2		−10	−10	34	13	−10	75
−10			19	28	190	−5	−0.2		−10	68	−10	13	−10	30
−10			−5	13	−20	−5	−0.2		−10	−10	13	−10	−10	−20
−10			257	20	34	−5	−0.2		−10	−10	−10	16	−10	−20
−10			−5	16	−20	−5	−0.2		−10	−10	−10	−10	−10	−20
−10			−5	52	−20	11	−0.2		−10	−10	−10	10	−10	−20
−10	−2	−10	17	82	59	−5	−0.2	3	−10	−10	35	50	13	−20
−10			32	43	36	−5	0.3		−10	−10	11	43	−10	−20
−10			32	201	564	−5	−0.2		−10	−10	11	38	−10	95
−10			98	148	230	−5	−0.2		−10	−10	20	50	−10	−20
−10	−2	10	40	188	872	38	0.5	2	−10	19	18	34	−10	−20
−10	−2	−10	24	38	59	5	−0.2	3	−10	−10	29	324	−10	25
−10	−2	13	−5	37	98	−5	−0.2	−2	−10	11	29	55	−10	−20
20			184	48	72	−5	6.3		−10	14	30	70	10	−20
−10			8	58	−20	−5	−0.2		−10	−10	12	−10	−10	−20
−10			−5	16	−20	30	−0.2		−10	−10	10	10	−10	965
−10			17	68	33	−5	−0.2		−10	−10	−10	−10	−10	−20
−10			7	15	−20	−5	−0.2		−10	−10	−10	−10	−10	−20
−10	−2	−10	8	22	43	5	−0.2	3	−10	−10	32	45	13	−20
−10			86	89	44	−5	−0.2		−10	−10	−10	60	−10	−20
−10	−2	21	26	10	−20	9	−0.2	−2		−10	21	47	−10	−20
−10			8	34	52	−5	−0.2		−10	−10	25	64	−10	−20
10	−2	88	232	408	212	28	−0.2	−2	−10	82	194	94	−10	−20
10	−2	−10	46	44	184	14	−0.2	2	−10	21	66	96	−10	−20
−10			23	49	21	−5	−0.2		−10	−10	15	25	−10	−20
−10			−5	20	−20	−5	−0.2		−10	−10	15	−10	−10	−20
18			123	114	86	−5	−0.2		−10	−10	−10	31	−10	−20
−10	−2	−10	147	39	222	−5	−0.2	2	−10	−10	19	41	−10	1500
−10			10	16	41	19	−0.2		−10	−10	−10	−10	−10	20
−10	−2	−10	145	31	77	6	−0.2	3	−10	10	28	52	−10	−20
10			48	42	−20	−5	−0.2		−10	−10	−10	−10	−10	−20
−10			−5	14	32	−5	−0.2		−10	−10	18	13	−10	−20
−10			359	117	301	−5	−0.2		−10	−10	−10	39	−10	325
−10	−2	22	1122	64	128	16	−0.2	−2	−10	23	36	44	−10	−20
			325	28	58	7	−0.2		−10	−10	−10	56	−10	20
−10			−5	32	36	−5	−0.2		−10	−10	14	−10	−10	−20
−10			26	70	376	−5	8.4		−10	32	16	−10	−10	−20
38	20	−10	164	342	1448	76	−0.2	−2	−10	128	28	28	−10	−20
−10			286	45	207	−5	−0.2		−10	−10	−10	113	−10	30
−10			37	28	54	−5	−0.2		−10	10	11	66	−10	−20

and less commonly as a stockwork; the stratiform layer immediately overlies the massive orebodies or occurs higher in the hanging-wall tuff. The Tetsusekiei are a mixed deposit with a clastic or tuffaceous component and a hydrothermal chemical component (chert, hematite, pyrite, chlorite, sericite, rutile, barite). The presence of abundant chlorite, sericite and hematite in the chemical component is reflected in the relatively low SiO_2 (< 59%) and high Al_2O_3 (up to 7.5%) and FeO_{total} (up to 33%); Cu, Zn and Pb nowhere exceed a few hundred ppm and Co and Ni even less. The rare-earth profiles of the two components are identical and represent the signature of the tuffaceous part. Kalogeropoulos and Scott (1983) consider the Tetsusekiei to form in three stages. The first takes place during maximum hydrothermal activity, with the formation of massive sulphides in a proximal position to the feeder vent and the deposition of the Tetsusekiei in a distal position through precipitation from the hydrothermal fluids. The second stage corresponds to a decrease in hydrothermal activity, enabling the deposition of only Tetsusekiei over the massive sulphides. This formation of an exhalite cover over the sulphides isolates the hydrothermal system from sea water and allows the temperature to increase; the third stage is one of recrystallization, with alteration of hematite to pyrite and the appearance of chalcopyrite disease (alteration of sphalerite to chalcopyrite). This phenomenon may occur several times, which explains the incorporation of an exhalite component within the sulphide body. Ohmoto et al. (1983), however, consider that the Tetsusekiei form from a slow mixing of hydrothermal fluids and cold sea water within sedimentary muds covering the massive sulphides, this occurring at both an early and a late stage in the hydrothermal activity.

Major differences in the chemico-mineralogical composition are noted with the South Iberian chert, which makes it rather difficult to compare these facies. The Tetsusekiei contain a major silico-aluminous phase which is absent, or only very slight, in the South Iberian chert. The Key Tuffite also contains a high proportion of

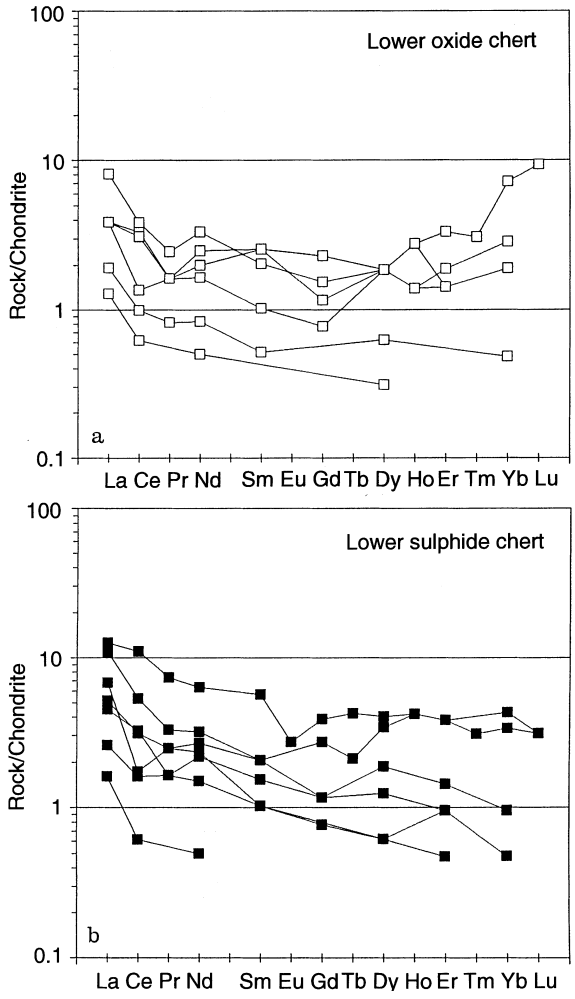

Fig. 9a, b Rare-earth plot of the **a** lower oxide chert and **b** lower sulphide chert

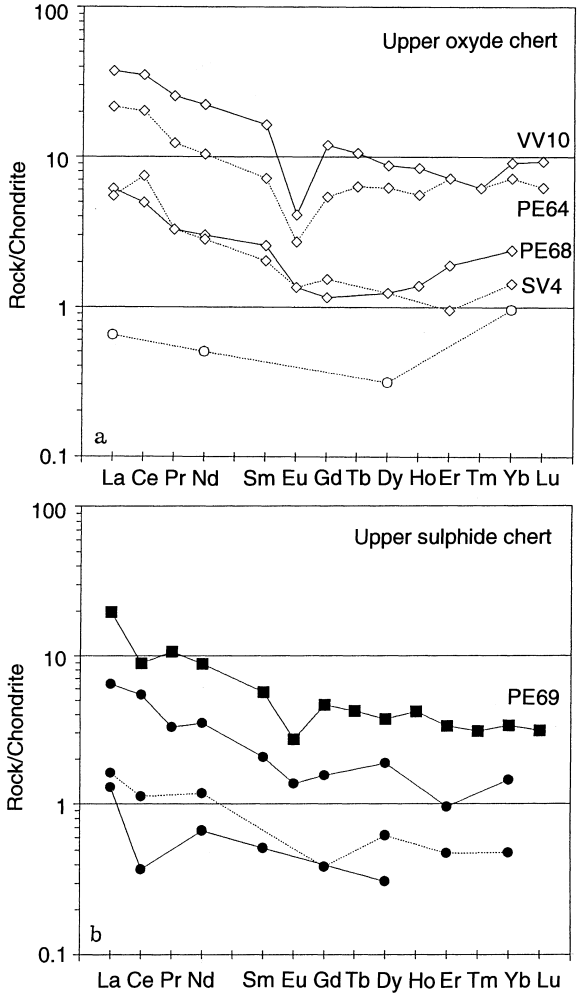

Fig. 10a, b Rare earth plot of the **a** upper oxide chert and **b** upper sulphide chert. *Sample numbers* are given for the radiolarian facies

tuffite which is reflected, among other indications, by the low silica content (40 to 52% SiO_2). Comparisons based on the major element and rare-earth contents are of little significance (Figs. 3 to 6). For the main metal elements, the Tetsusekiei normalized diagram (proposed by Urabe and Kusakabe, 1990; Fig. 13) mainly emphasizes the generally high Mn content of the South Iberian chert and its lower Fe-Ba-Pb content. The other elements, such as Zn-Cu-As-Sb, show comparable but variable concentrations. The South Iberian chert therefore appears as a clearly different facies from the hydrothermally altered tuffaceous layers considered as lateral markers of the Kuroko or Abitibi type massive sulphides. As such it seems to be more comparable with the silica iron exhalites from the Mount Windsor volcanic belt (Australia).

Silica iron exhalites (*Mount Windsor volcanic belt, Australia*)

Silica iron exhalites are common in the Mount Windsor volcano-sedimentary succession hosting the Thalanga massive sulphide deposit (Berry et al. 1992) and have been studied in detail (Duhig et al. 1992). The exhalites are found at three stratigraphic levels in the succession relative to the Thalanga deposit; below, above, and laterally equivalent to the deposit. Clasts of silica iron exhalite are present in the massive sulphides and a quartz-barite-magnetite facies caps the orebody, although its relationships with the exhalites have yet to be established. Duhig et al. (1992) consider the exhalites to have crystallized from gels accumulated in topographic depressions and to result from the mixing of sea water with a low-temperature (10 to 40 °C) hydrothermal fluid; the fluid could have derived from a weak in situ hydrothermal activity or represent the distal relict of

►

Fig. 11a, b Rare-earth plot of **a** Aljustrel type chert (with *sample numbers*) and **b** chert from outside the Iberian Pyrite Belt: *squares*: Cenozoic radiolarian chert from the Deep Sea Drilling Project (DSDP); *diamonds*: Kamiasô Permian-Jurassic radiolarian chert (Gifu, Japan) after Shimizu and Masuda (1977); circles: Cambrian silica iron exhalites from the Mount Windsor volcanic belt (Australia) after Duhig et al. (1992)

Table 2 Lead isotope ratios for the South Iberian chert. 1: red hematitic chert; 2: red hematitic chert with magnetite; 3: red conglomeratic chert with hematite; 4: grey sulphidic chert with hematitic elements; 5: grey sulphidic chert; 6: grey chert without sulphide. All ratios are corrected to t = 351 Ma

Sample	$^{206}Pb/^{204}Pb$	$^{207}Pb/^{204}Pb$	$^{208}Pb/^{204}Pb$	U (ppm)	Pb (ppm)	μ	Location	Type
CO41	18.320	15.616	38.381	5.97	68	2.38	Los Enjambres	1
CO44	18.514	15.649	38.275	6.23	31	1.77	San Platón	1
CV3	18.240	15.628	38.105	3.61	41	5.69	Embalse del Alisal	1
PE64	18.237	15.615	38.230	5.95	400	0.95	Peña de Hierro – Los Ermitanos	1
95B	18.208	15.611	38.213	2.25	37	3.88	El Chaparral	2
OD11a	18.679	15.722	39.004	2.01	51	2.55	Odiel Asperon	2
PE74	18.106	15.635	38.255	1.57	33	0.42	Campofrio	2
SV4	18.477	15.653	38.486	1.61	20	9.29	Soloviejo	3
24a	18.266	15.641	38.357	0.46	1203	0.02	La Torerera	4
26d	18.251	15.623	38.326	1.45	565	0.16	Rio Odiel	4
PE69	18.445	15.604	38.516	1.56	62	1.60	Porto Alegre	4
024	18.260	15.627	38.323	2.04	2224	0.06	Los Guijos 2	5
287C	18.293	15.629	38.364	0.25	744	0.02	Santiago	5
485B	18.237	15.634	38.304	2.59	3962	0.04	El Cuervo	5
8b	18.167	15.622	38.302	9.17	177	0.70	Morante	5
AJ1	18.237	15.611	38.265	4.52	99	2.90	Aljustrel Feitais	5
VL1	18.278	15.628	38.305	2.04	333	0.39	Vallejin	5
6a	18.526	15.653	38.234	2.59	117	1.42	Morante	6
PE71	18.210	15.626	38.280	7.37	380	1.24	Porto Alegre	6

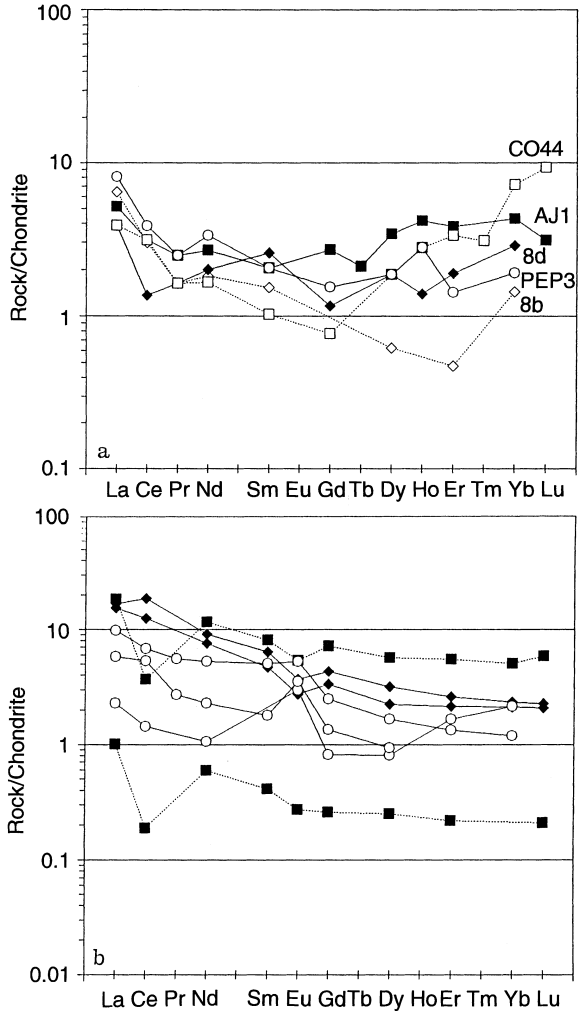

fluids that had already deposited the massive sulphides. Microorganisms (bacteria and/or fungi) played an important role in oxidizing Fe^{2+} to Fe^{3+}. Finally, these siliceous deposits could have formed at all stages during the activity of the hydrothermal system; i.e. early, contemporaneous or late with respect to the precipitation of the Thalanga massive sulphides. From their variable stratigraphic position, their macroscopic appearance, their petrography, their major-element chemical composition and their weak LREE enrichment (notably very weak positive and negative Ce anomalies; Fig. 11b), the Mount Windsor silica iron exhalites are in every respect comparable to the oxide chert of the Iberian Pyrite Belt. The Australian facies are distinguished by (a) a paucity

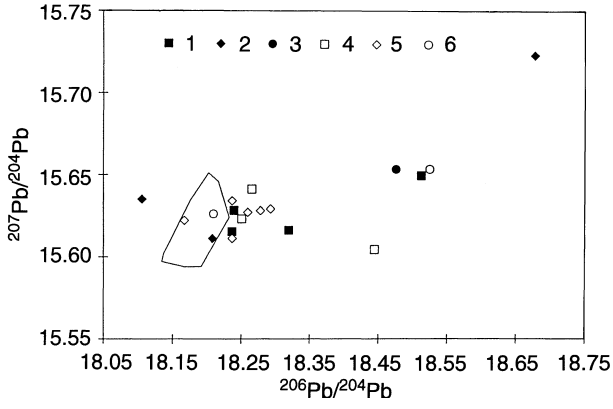

Fig. 12 $^{206}Pb/^{204}Pb$ versus $^{207}Pb/^{204}Pb$ plot of South Iberian chert and sulphide mineralization. *1*: red hematitic chert; *2*: red hematitic chert with magnetite; *3*: red conglomeratic hematitic chert; *4*: grey sulphidic chert with hematitic elements; *5*: grey sulphidic chert; *6*: grey chert without sulphide; *Contoured area*: massive sulphide deposits, after Marcoux (1997)

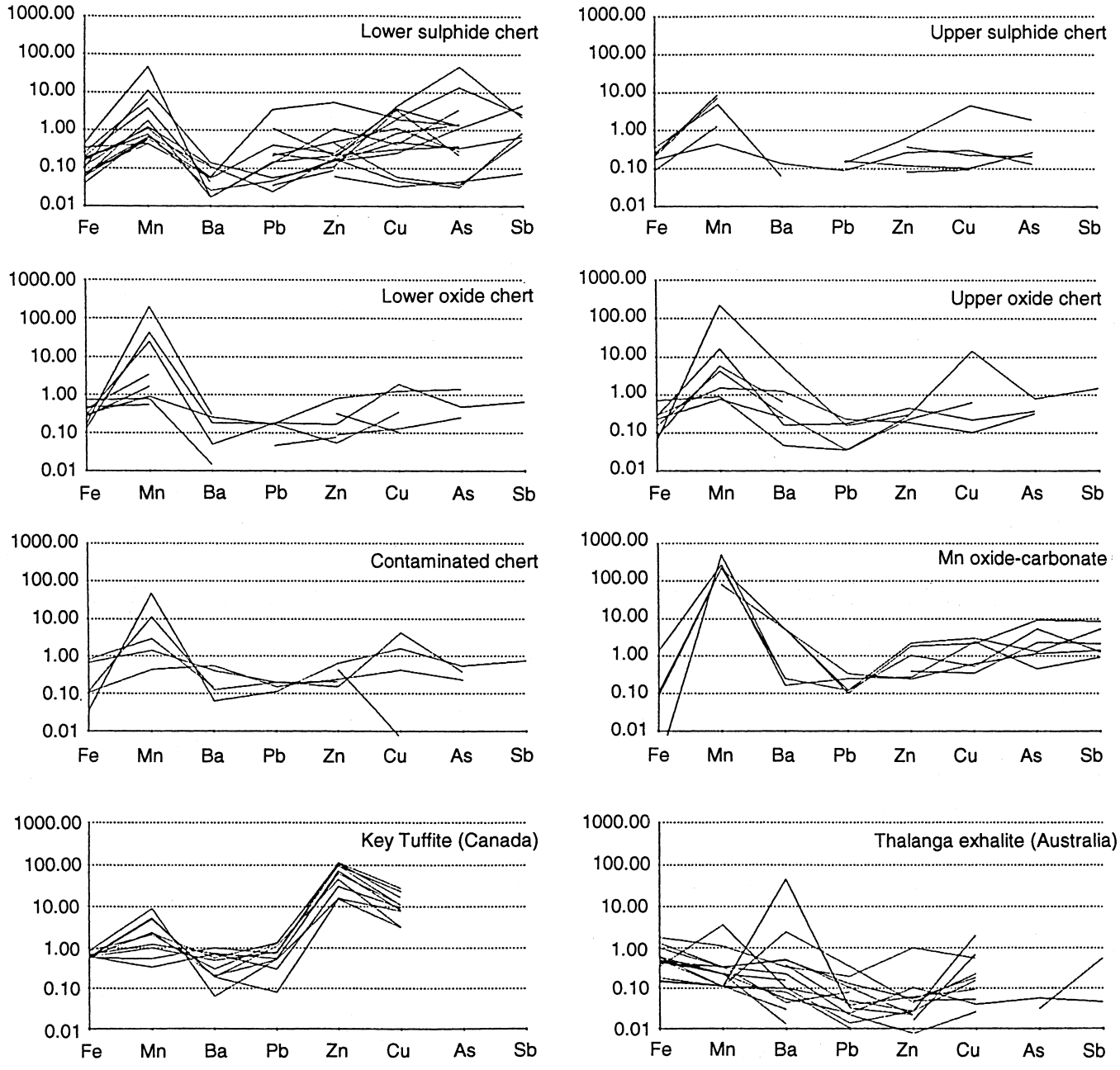

Fig. 13 Tetsusekiei normalization diagram (after Urabe and Kusabe 1990) showing the South Iberian chert, the Key Tuffite (Matagami, Canada, after Liaghat and MacLean 1992) and the silica iron exhalites from the Mount Windsor volcanic belt (Australia, after Duhig et al. 1992). *Fe*, Fe total

of sulphides (apparent absence of the pale silica + sulphide phase), (b) low manganese and high barium contents (Fig. 13), and (c) marked positive Eu anomalies (Fig. 11b) that are interpreted as reflecting an Eu enrichment of the hydrothermal fluids through reaction with the plagioclase of the percolated country rock.

A comparison of South Iberian chert with some facies of present-day sub-marine hydrothermal mineralizations is not convenient. Present-day hydrothermal Fe-Si deposits are described (Hekinian et al. 1993) and Mn encrustations linked with sulphide mineralization are pointed out (Usui and Nishimura 1992a,b). But siliceous facies equivalent to the South Iberian chert have not been discovered to our knowledge.

Palaeogeography

Research carried out on the volcanism of the Iberian Pyrite Belt has established that the depositional environment was shallow marine ("just at water level"; Routhier et al. 1980), which confirms our own field observations of the volcanic and sedimentary rocks. The presence of radiolarians is not a determining element because, although they are commonly considered as markers of a siliceous environment at great depth, they

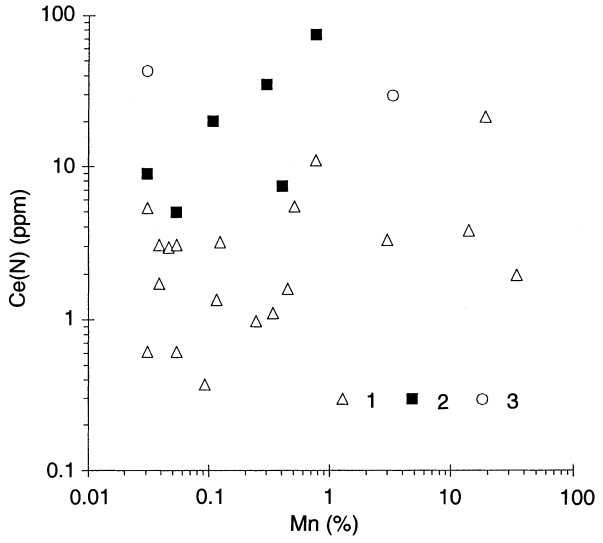

Fig. 14 Mn versus $(Ce)_N$ plot of the South Iberian chert; the chert (other than the radiolarian chert and contaminated chert) shows a weak positive correlation; the same correlation would be seen on a Mn versus ΣLREE diagram. *1*: chert; *2*: radiolarian chert; *3*: contaminated chert

can also proliferate when the environment is enriched in silica even in relatively shallow water, as is well known in outer shelf environments at depths of 100 to 250 m. The acidic volcanic activity, for which there is a superabundance of indications in the Iberian Pyrite Belt, would have been sufficient to produce such silica enrichment (C. Bourdillon BRGM, written communication).

Shimizu and Masuda (1977) show that recent deep-sea cherts are marked by a strong negative Ce anomaly (Ce/Ce* = 0.2 to 0.3) characteristic of the type of environment. They also show that old fossil cherts (Permian-Jurassic in Japan, Archean in Canada) give a weak positive Ce anomaly (Ce/Ce* > 1) which reflects a shallow marine environment. The rare-earth profiles of the South Iberian chert are clearly different from those of recent deep-sea cherts, but are in all respects comparable with those of the old fossil cherts presented by Shimizu and Masuda (1977) (Figs. 6 and 11b). The South Iberian chert generally shows weak positive Ce anomalies (Ce/Ce* = 1.16 to 1.38), which could thus indicate a shallow marine environment.

This type of approach is also used by Pracejus et al. (1990), who refer to the strong positive Ce anomaly of marine ferromagnesian oxides, accompanied by a higher rare-earth content than is found in chondrites or NASC (see also Haskin and Haskin 1966; Piper 1974). Shallow continental shelf and epicontinental sea deposits have lower rare-earth contents and a very weak or absent Ce anomaly. Normalizing the South Iberian chert to NASC effectively reveals their lower rare-earth content (by a factor between 1 and 10^{-1}), which again would indicate a shallow water environment.

Present-day submarine hydrothermal mineralizations are known only at depth greater than 900 m (Ishibashi adn Urabe 1995), and it is well known that an important water column is necessary to prevent the fluid from boiling (a condition for metal conservation). This contradiction still needs to be resolved.

Origin of the South Iberian chert

With high Fe-Mn and low Co + Ni + Cu (< 400 ppm), the chert facies and associated rocks of the Iberian Pyrite Belt can be considered as hydrothermal (as opposed to "hydrogenous", according to the classification of Bonatti et al. 1972, Fig. 3). In this we agree with the conclusions of Barriga and Oliveira (1986) and Barriga (1986).

The geochemical behaviour of rare earths is strongly influenced by hydrothermal processes (see Lottermoser 1992, for a review and discussion of this aspect). The submarine hydrothermal fluids of the East Pacific Rise (EPR) type are clearly enriched in LREE and Eu, as are the pure hydrothermal precipitations of the Red Sea deposits; the Green Seamount hydrothermal sediments also show a clear Eu enrichment. Hydrothermal sediments are equally characterized both by their content in precious metals, base metals and associated elements (As, Sb, Tl, Ba, Co, Se, Cd) and by their content in rare earths of the same type as contained by the hydrothermal fluids. As against this, the distribution of rare earths (negative Ce anomaly and weak negative Eu anomaly) and the trace-element and base-metal contents of the Fe-Mn sediments that precipitate on all ocean floors are similar to those of sea water, although obviously with much higher concentrations. The two types of fluid, sea water and hydrothermal fluid, thus have distinctive rare-earth profiles that are imparted to their associated sediments. The fact that positive Eu anomalies are common in sulphide ores and their associated chemical precipitates is interpreted as due to a reaction of the convective sea water with the acidic country rock containing Eu-enriched feldspars. The hydrothermally altered volcano-sedimentary pile can thus show an impoverishment in Eu and, further away from the mineralized mass, the chemical precipitates can show a very clear drop in Eu content (such as at Broken Hill).

From the rare-earth geochemistry of the hematitic chert overlying the Feitais massive sulphide deposit (Aljustrel) and from the oxygen isotopic measurements of the quartz separated out from this chert ($\delta^{18}O$ between +17.9 and 20.1‰) and from massive rhodonite (Mértola, $\delta^{18}O$ = 14.8‰) it can be concluded that the chert formed through precipitation from a hydrothermal fluid dominated by sea water at temperatures of between 110 and 130 °C (Barriga and Kerrich 1984 ; Munhá et al. 1986 ; Barriga and Fyfe 1988). The highly negative $\delta^{34}S$ values of pyrite disseminated in the chert (between −7.6 and −31.6‰), as opposed to the positive values (between 0 and +10‰) measured in the massive-sulphide-type mineralization, indicate a bacterial reduction in the sulphate-rich marine environment with a fairly strong fractionation (Routhier et al. 1980).

Our own rare-earth analyses of the South Iberian chert give cerium anomalies that are variable (positive or negative) and weak and europium anomalies that appear to be weakly negative. Our samples do not show the characteristics mentioned by Barriga and Fyfe (1988), but it should be noted that the published analytical data on Gaviao (another orebody at Aljustrel) also indicate weak and variable (negative to positive) cerium anomalies, although with europium anomalies that can be strongly positive (Relvas 1991). The absence of a well-marked negative cerium anomaly means that we do not have the clear signature of a fluid dominated by sea water, and the absence of positive europium anomaly (in our samples) distinguishes the South Iberian chert from both the Red Sea type submarine metalliferous hydrothermal sediments and the EPR type hydrothermal fluids. However, the EPR type fluids are acidic (pH < 6) and high temperature ($T > 230$ °C) and their composition is independent of the country rocks through which they percolate, whereas the rare-earth composition of the lower temperature (< 100 °C) acidic fluids shows a much lower concentration clearly influenced by the country rocks that they have crossed (Michard 1989). A similar country rock influence can be envisaged for the South Iberian chert, notably to explain the observed variation in cerium content. Where the country rock has been totally altered through silicification, it is possible that the REE content was affected by that of the initial rock.

Recent data on present-day submarine hydrothermal Fe-Mn-Si oxide deposits of the Franklin Seamount (Woodlark Basin, Papua-New Guinea) show very flat rare-earth spectra with weakly negative cerium anomalies and no marked europium anomaly (Binns et al. 1993). Other present-day hydrothermal Fe-Si oxyhydroxide deposits of the East Pacific Rise and nearby areas (Society Islands, Austral Islands, Pitcairn area) also show variable cerium and europium anomalies (Hekinian et al. 1993). The participation of sea water through mixing with the hydrothermal fluids can therefore only be considered where the spectra show negative Ce and Eu anomalies; the presence of positive Ce anomalies is thus interpreted as reflecting a preferential incorporation of Ce^{4+} from sea water in the Mn-Fe oxide deposits, whereas the positive Eu anomalies mark the circulation of high-temperature fluids (Hekinian et al. 1993). In South Iberia, the Mn versus ΣLREE and Mn versus $(Ce)_N$ correlations are positive, albeit imperfect, if one excludes the radiolarian chert and contaminated chert (Fig. 14); this reflects a limited trapping of LREE, especially Ce, by Mn oxides which would not, in any case, be very abundant in the primary deposits. As against this, ΣLREE shows a positive correlation with Fe^{2+} (Fig. 15a) and a negative correlation with Fe^{3+} (Fig. 15b), indicating that the iron oxidation was not accompanied by enrichment in LREE as has been described for the "hydrogenous" Fe-Mn encrustations of the sea floor (Bonatti 1975; Bonatti et al. 1976). Similarly, there is no correlation between Mn and the Fe^{3+}/Fe^{2+} ratio, which suggests that the LREE enrichment, and particularly that of Ce, is not due to fractionation of Mn with respect to Fe.

The variability of the rare-earth profiles could thus reflect a trapping of sea-water LREE through formation of manganese oxides and/or an influx of low-temperature hydrothermal fluids having percolated through the country rocks of the volcano-sedimentary succession. The pale sulphidic siliceous facies affects the red hematitic facies from the base up through percolation or brecciation; this position, combined with the evolution of an oxide facies towards a sulphide facies, indicates an absence of direct contact with sea water. The cerium enrichment of the sulphide facies would therefore tend to reflect a contribution from hydrothermal fluids rather than a "scavenging" of sea water. The absence of positive Eu anomaly in our samples would indicate that the studied chert deposits were produced without notable influence from the metalliferous hydrothermal fluids giving rise to the massive sulphide mineralization. This is confirmed by the lead isotopic composition of the chert,

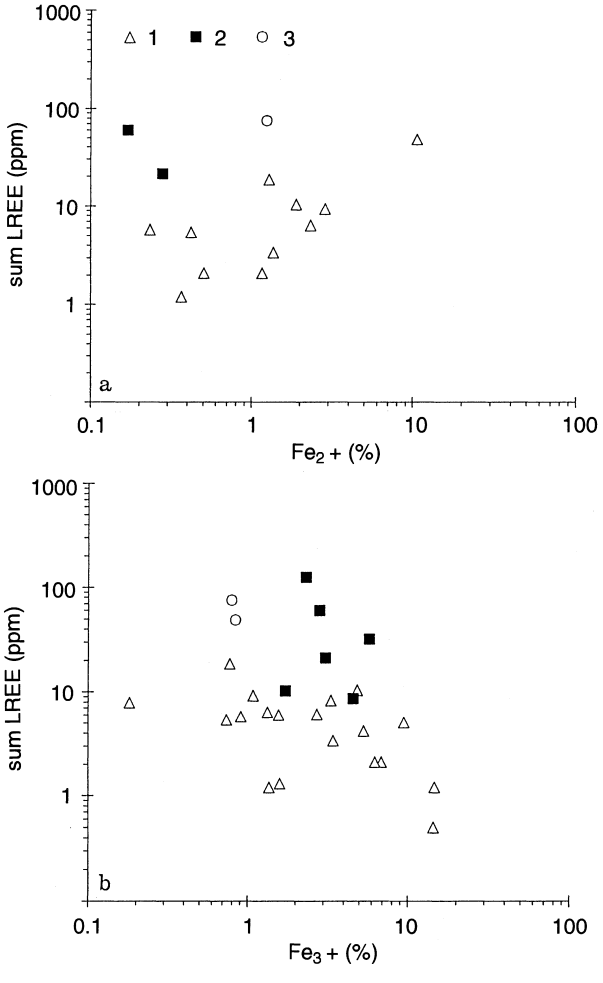

Fig. 15a ΣLREE versus Fe^{2+}, and **b** ΣLREE versus Fe^{3+} plots of the South Iberian chert. *1*: chert; *2*: radiolarian chert; *3*: contaminated chert

which is more radiogenic than that of the massive sulphides.

The hydrothermal activity that gave rise to the sulphide chert facies seems to us, therefore, as diverging from that responsible for the massive sulphide mineralization. At a same site, one may clearly distinguish the evolution [oxide chert → sulphide], but nowhere does one see the passage [sulphide chert → massive sulphide type mineralization].

Conclusions

The South Iberian chert is of hydrothermal origin and was formed in a shallow marine environment, shelf or epicontinental sea according to the volcanological, sedimentological and geodynamic data. Two main stratigraphic chert-bearing levels are distinguished; a lower level at the top of the lower acidic volcanics (VA1) or in the associated sediments, and an upper level at the top of the upper volcanics (VA2) and in places directly associated with the purple schist marker horizon. Four facies types are recognized: (1) red hematitic chert ± magnetite; (2) radiolarian and/or sedimentary-textured chert with hematite and/or Mn oxide; (3) pale sulphidic chert; (4) rhodonite and/or Mn carbonate ± magnetite facies. In the Spanish part of the Province, the radiolarian chert is restricted to the upper level, whereas the distribution of the other facies appears to be haphazard.

The chert was emplaced below the sea floor through chemical precipitation and/or alteration and replacement of the country rock. The oxide facies formed first, possibly creating a protective cover from the marine environment and allowing evolution towards the sulphide facies; the Mn carbonate and silicate + quartz ± chlorite and sulphide phase occurred even later. Our field observations and geochemical data show the independence of this siliceous sulphide hydrothermal event with respect to the hydrothermal fluids giving rise to the massive sulphides, and no discrimination has so far enabled us to isolate a chert that could be a direct lateral marker of the massive sulphide deposits. This is well illustrated by the lead isotopic signature of the chert, which is notably more radiogenic than that of the massive sulphides; the sulphidic chert facies show an enrichment in lead which source (sediments, sea water) is different from the source lead of the massive sulphides (see Marcoux 1997). The hypothesis of an independent hydrothermal "chert" event (or even several events) can thus be envisaged; the chert would mark low-temperature submarine hydrothermal activity that was probably fairly continuous, but which becomes particularly visible during a "break" within the volcano-sedimentary succession. Under this hypothesis, the chert would not represent a lateral equivalent *sensu stricto* of the massive sulphide deposits; its exploration value resides in its palaeodynamic significance as a marker of volcanic quiescence or absence of volcanism in some part of the basin, i.e. a suitable time or place for the deposition of massive sulphides. It is also logical that, in certain cases, the low-temperature hydrothermal "chert" activity and the higher temperature hydrothermal "massive sulphide" activity would be in competition, with the chert capable of locally favouring the underlying development of massive sulphides through providing a protective insulating cap.

Acknowledgements This study was carried out as part of a scientific research project on the South Iberian massive sulphide deposits and their geological setting, cofinanced in part by the European Community (CE-DGXII contracts MA2M-CT90-0029 and BRE2-CT92-0299). We are particularly grateful to our BRGM colleagues who have helped us to realize this work, and in particular to C. Bourdillon for her study of the radiolarians, J.L. Lescuyer and P. Piantone for their critical review of the manuscript, and Sir Patrich Skipwith Bt. for his translation of this paper. We acknowledge gratefully A. Arribas and T. Urabe, reviewers of Mineralium Deposita.

References

Barriga FJAS (1986) Lithogeochemistry and petrography as exploration tools in the Iberian pyrite belt: the Aljustrel example. II Congr Nacion Geol, 29 Sept–2 Oct. 1986, University of Lisboa, Abstr, Maleo Bol Inform Soc Geol Port 2(13): p 11

Barriga FJAS (1990) Metallogenesis in the Iberian pyrite belt. *In:* Dallmeyer RD, Martínez García E(eds) Pre-Mesozoic geology of Iberia. Springer-Verlag, Berlin Heidelberg New York, pp 369–379

Barriga FJAS, Fyfe WS (1988) Giant pyritic base-metal deposits: the example of Feitais (Aljustrel, Portugal). Chem Geol 69: pp 331–343

Barriga FJAS, Kerrich R (1984) Extreme $^{(18)}$O-enriched volcanics and $^{(18)}$O-evolved marine water, Aljustrel, Iberian pyrite belt; transition from high to low Rayleigh number convective regimes. Geochim Cosmochim Acta 48(5): 1021–1031

Barriga FJAS, Oliveira JT (1986) Geochemical study of cherts, jaspers and manganese ores from the Iberian pyrite belt. II Congr Nacion Geol 29 Sept–2 Oct. 1986, University of Lisboa, Abstr, Maleo Bol Inform Soc Geol Port 2(13): p 11

Berry RF, Huston DL, Stolz AJ, Hill AP, Beams SD, Kuronen U, Taube A (1992) The stratigraphy, structure, and mineralization of the Mount Windsor subprovince, north Queensland, Australia. Econ Geol 87: 739–763

Binns RA, Scott SD, Bogdanov YA, Lisitzin AP, Gordeev VV, Gurvich EG, Finlayson EJ, Boyd T, Dotter LE, Wheller GE, Muravyev KG (1993) Hydrothermal oxide and gold-rich sulfate deposits of Franklin Seamount, Western Woodlark Basin, Papua New Guinea. Econ Geol 88: 2122–2153

Bonatti E (1975) Metallogenesis at oceanic spreading centers. Annu Rev Earth Planet Sci Lett 3: 401–431

Bonatti E, Kraemer T, Rydell H (1972) Classification and genesis of submarine iron-manganese deposits. *In:* Horn D (ed), Ferromanganese deposits on the ocean floor. National Science Foundation, Washington D.C., pp 149–165

Bonatti E, Zerbi M, Ray R, Rydell H (1976) Metalliferous deposits from the Appenine ophiolites: Mesozoic equivalents of modern deposits from oceanic spreading centers. Geol Soc Am Bull 87: 83–94

Bostrom K (1973) The origin and fate of ferromanganoan active ridge sediments: Stockholm. Contr Geol 27: 19–243

Boulègue J, Perseil EA, Bernat M, Dupré B, Stouff P, Francheteau J (1984) A high-temperature hydrothermal deposit on the East Pacific Rise near 7°N. Earth Planet Sci Lett 70: 249–259

Brévart O, Dupré B, Allègre CJ (1981) Metallogenesis at Spreading centers: lead isotope systematics for sulfides, manganese-rich crusts, basalts, and sediments from the Cyamex and Alvin areas (East Pacific Rise). Econ Geol 76: 1205–1210

Carvalho D (de), Conde L, Hernández Enrile J, Oliveira V, Schermerhorn LJGS (1976) Livro-guia das excursoes geologicas na faixa piritosa ibérica. III Reun geol SO Maciço Hespérico da Península Ibérica, Huelva – Beja, Faixa piritosa Ibérica. *In*: Comun Serv Geol Port LX: 271–315

Dallmeyer RD, Martínez García E (1990) Introduction to the Pre-Mesozoic geology of Iberia. *In:* Dallmeyer RD Martínez García E (eds) Pre-Mesozoic geology of Iberia Springer-Verlag, Berlin Heidelberg New York, pp 3–4

Davidson AJ (1977) Petrography and chemistry of the Key Tuffite at Bell Allard, Matagami, Quebec. MSc Thesis, McGill University, Montreal, Quebec, Canada, 131 p

Duhig NC, Stolz J, Davidson GJ, Large RR (1992) Cambrian microbial and silica gel textures in silica iron exhalites from the Mount Windsor volcanic belt, Australia: their petrography, chemistry, and origin. Econ Geol 87: 764–784

Franklin JM, Lydon JW, Sangster DF (1981) Volcanic-associated massive sulfide deposits. Econ Geol 75th Anniv Vol, pp 485–627

Garcia Palomero F (1990) Rio Tinto deposits. Geology and geological models for their exploration and ore reserves evaluation. *In*: Sulphide deposits – their origin and processing, Institute of Mining Metallurgy, pp 17–35

Haskin MA, Haskin LA (1966) Rare-earth elements in European shales: a redetermination. Science 154: 507–509

Henderson P (1984) Rare earth element geochemistry. Development in geochemistry 2. Henderson P (ed) Elsevier, Amsterdam 510 p

Hekinian R, Hoffert M, Larqué P, Cheminée JL, Stoffers P, Bideau D (1993) Hydrothermal Fe and Si oxyhydroxide deposits from South Pacific intraplate volcanoes and East Pacific Rise axial and off-axial regions. Econ Geol 88: 2099–2121

Ishibashi J, Urabe T (1995) Hydrothermal activity related to arc-backarc magmatism in the Western Pacific. *In*: Taylor B (ed) Backarc basins: tectonics and magmatism. Plenum Press, N.Y., pp 451–495

Kalogeropoulos SI, Scott SD (1983) Mineralogy and geochemistry of tuffaceous exhalites (Tetsusekiei) of the Fukasawa mine, Hokuroko district, Japan. Econ Geol Monogr 5: 412–432

Klau W, Large DE (1980) Submarine exhalative Cu-Pb-Zn deposits, a discussion of their classification and metallogenesis. Geol Jahrb D 40: 13–58

Large RR (1977) Chemical evolution and zonation of massive sulfide deposits in volcanic terrains. Econ Geol 72: 549–572

Leca X, Ribeiro A, Oliveira JT, Silva JB, Albouy L, Carvalho P, Merino H (1983) Cadre géologique des minéralisations de Neves Corvo, Baixo Alentejo, Portugal. Mém BRGM 121, 79 p

Leca X, Albouy L, Aye F, Picot P (1985) Caractéristiques principales du gisement de Neves-Corvo (Portugal) Chron Rech Min 481: 53–58

Leistel JM, Bonijoly D, Braux C, Freyssinet P, Kosakevitch A, Leca X, Lescuyer JL, Marcoux E, Milési JP, Piantone P, Sobol F, Tegyey M, Thiéblemont D, Viallefond L (1994) The massive sulphide deposits of the South Iberian Pyrite Province: geological setting and exploration criteria. Doc BRGM 234, 236 p

Leistel JM, Marcoux E, Thiéblemont D, Quesada C, Sánchez A, Almodovar GR, Pascual E, Sáez R (1998) The volcanic-hosted massive sulphide deposits of the Iberian Pyrite Belt: Review and preface to the Thematic issue. Mineralium Deposita 33: 2–30

Liaghat S, MacLean WH (1992) The Key Tuffite, Matagami mining district: origin of the tuff components and mass changes. Explor Mini Geol 1 (2): 197–207

Lottermoser BG (1992) Rare earth elements and hydrothermal ore formation processes. Ore Geol Rev 7: 25–41

Marcoux E (1998) Lead isotope systematics of the giant massive sulphide deposits in the Iberian Pyrite Belt. Mineralium Deposita 33: 45–58

Marcoux E, Leistel JM, Sobol F, Milési JP, Lescuyer JL, Leca X (1992) Signature isotopique du plomb des amas sulfurés de la province de Huelva, Espagne. Conséquences métallogéniques et géodynamiques. CR Acad Sci Fr 314, ser II: 1469–1476

Michard A (1989) Rare earth element systematics in hydrothermal fluids. Geochim Cosmochim Acta 53: 745–750

Munhá J (1983) Hercynian magmatism in the Iberian pyrite belt. *In*: Lemos de Souza J, Oliveira JV (eds) The Carboniferous of Portugal. Mem Serv Geol Port 29: 39–81

Munhá J, Barriga FJAS, Kerrich R (1986) High $^{(18)}$O ore-forming fluids in volcanic-hosted base metal massive sulfide deposits: geologic, $^{(18)}$O/$^{(16)}$O, and D/H evidence from the Iberian pyrite belt; Crandon, Wisconsin; and Blue Hill, Maine. Econ Geol 81 (3): 530–552

Oehler JH (1976) Hydrothermal crystallisation of silica gel. Geol Soc Am Bull 87: 1143–1152

Ohmoto H, Mizukami M, Drummond SE, Eldridge CS, Pisutha-Arnond V, Lenagh TC (1983) Chemical processes of Kuroko formation. Econ Geol Monogr 5: 570–604

Oliveira JV (1990) South Portuguese Zone: (1) Introduction, (2) Stratigraphy and synsedimentary tectonism. *In*: Dallmeyer RD Martínez Garcia E (eds) Pre-Mesozoic geology of Iberia. Springer-Verlag, Berlin Heidelberg New York, pp 333–347

Pinedo Vara I (1963) Piritas de Huelva – Su historia, minería y aprovechamiento. Ed. Summa, Madrid, 1003 p

Piper DZ (1974) Rare-earth elements in the sedimentary cycle: a summary. Chem Geol 14: 285–304

Pracejus B, Bolton BR, Frakes LA, Abbott M (1990) Rare-earth element geochemistry of supergene manganese deposits from Groote Eylandt, Northern Territory, Australia. Ore Geol Rev 5: 293–314

Rahders E, Germann K (1993) Distribution and origin of gold and silver in host rocks of volcanogenic massive sulphide and manganese deposits in the Pyrite Belt of Southern Spain. *In*: Fenoll Hach-Alí P, Torres-Ruiz J, Gervilla F (eds) Current research in geology applied to ore deposits. Proc 2nd Biennal SGA Meeting, Granada, Spain, Sept. 9–11, 1993, pp 373–375

Relvas J (1991) Estudo geológico e metalogenético da área de Gaviao, Baixo Alentejo. Thesis, University of Lisbon, 250 p

Roberts RG (1975) The geological setting of the Mattagami Lake Mine, Quebec: a volcanogenic massive sulfide deposit. Econ Geol 70: 115–129

Roy S (1981) Manganese deposits. Academic Press, Harcourt Brace Jovanovich Publishers, 458 p

Routhier P, Aye F, Boyer C, Lécolle M, Molière P, Picot P, Roger G (1980) La ceinture sud-ibérique à amas sulfurés dans sa partie espagnole médiane. Tableau géologique et métallogénique. Synthèse sur le type amas sulfurés volcano-sédimentaires. 26th Int Geol Congr, Paris, Mém BRGM, France, 94, 265 p

Sáez R, Almodóvar GR (1993) An introduction to the ore geology of the Iberian Pyrite Belt. *In*: Fenoll Hach-Alí P, Torres-Ruiz J, Gervilla F, Velasco F (eds) Current research in geology applied to ore deposits, Field trip guide of the 2nd Biennal SGA Meeting, Granada, Spain, Sept. 9–15, 1993, pp 1–17

Schermerhorn LJG (1971) An outline stratigraphy of the Iberian pyrite belt. Bol Geol Min Spain 82: 238–268

Scott SD, Kalogeropoulos SI, Shegelski RJ, Siriunas JM (1983) Tuffaceous exhalites as exploration guides for volcanogenic sulphide deposits. J Geochem Explor 19: 500–502

Shanks WC, Boehlke JK, Seal RR (1995) Stable isotopes in mid-ocean ridge hydrothermal systems: interaction between fluids, minerals, and organisms. *In*: Humphris S et al. (eds) Seafloor hydrothermal systems. Geophys Monogr 91: 194–221

Shimizu H, Masuda A (1977) Cerium in chert as an indication of marine environment of its formation. Nature 266: 346–348

Silva JB, Oliveira JV, Ribeiro A (1990) South Portuguese zone. Structural outline. *In*: Dallmeyer RD Martínez García E (eds) Pre-Mesozoic Geology of Iberia. Springer-Verlag, Berlin Heidelberg New York, pp 348–362

Strauss GK (1970) Sobre la geología de la provincia piritifera del Suroeste de la Península Ibérica y de sus yacimientos, en especial sobre la mina de pirita de Lousal, Portugal Mem Inst Geol Min Esp 77: 266 p

Strauss GK, Beck JS (1990) Gold mineralisations in the SW Iberian pyrite belt. Mineralium Deposita 25(4): 237–245

Strauss GK, Madel J (1974) Geology of massive sulphide deposits in the Spanish – Portuguese pyrite belt. Geol Rundsch 63: 191–211

Thiéblemont D, Tegyey M, Marcoux E, Leistel JM (1994) Genèse de la province pyriteuse sud-ibérique dans un paléo-prisme d'accrétion ? Arguments pétrologiques. Bull Soc géol Fr 165(5): 407–423

Urabe T, Kusakabe M (1990) Barite silica chimneys from the Sumisu Rift, Izu-Bonin arc: possible analog to hematitic chert associated with Kuroko deposits. Earth Planet Sci Lett 100: 283–290

Usui A, Nishimura A (1992a) Submersible observation of hydrothermal manganese deposits on the Kaikata Seamount, Izu-Ogasawara (Bonin) Arc Mar Geol 106: 203–216

Usui A, Nishimura A (1992b) Hydrothermal manganese oxide deposits from Izu-Ogasawara (Bonin)-Mariana Arc and adjacent areas. Bull Geol Surv Japan 43: 257–284

Wonder JD, Spry PG, Windom KE (1988) Geochemistry and origin of manganese-rich rocks related to iron-formation and sulfide deposits, Western Georgia. Econ Geol 83: 1070–1081